Mammalian bone palaeohistology: new data on island forms and a survey

Christian Kolb, Torsten M. Scheyer, Kristof Veitschegger, Analia M. Forasiepi, Eli Amson, Alexandra A E van der Geer, Lars W. van den Hoek Ostende, Shoji Hayashi, Marcelo R. Sánchez-Villagra

The interest in mammalian palaeohistology has increased dramatically in the last two decades. Starting in 1849 via descriptive approaches, it has been demonstrated that bone tissue and vascularisation types correlate with several biological variables such as ontogenetic stage, growth rate, and ecology. Mammalian bone displays a large variety of bone tissues and vascularisation patterns reaching from lamellar or parallel-fibred to fibrolamellar or woven-fibred bone, depending on taxon and individual age. Here we systematically review the knowledge and methods on cynodont and mammalian bone as well as palaeohistology and discuss potential future research fields and techniques. We present new data on the bone microstructure of two extant marsupial species and of several extinct continental and island placental mammals. Recent marsupials display mainly parallel-fibred primary bone with radial, oblique, but mainly longitudinal vascular canals. Three juvenile specimens of the dwarf island hippopotamid *Hippopotamus minor* from the Late Pleistocene of Cyprus show reticular to plexiform fibrolamellar bone. The island murid *Mikrotia magna* from the Late Miocene of Gargano, Italy displays parallel-fibred primary bone with reticular vascularisation and compact coarse cancellous bone in the central part of the cortex. *Leithia* sp., the dormouse from the Pleistocene of Sicily, is characterised by a primary bone cortex consisting of lamellar bone and low vascularisation. The bone cortex of the fossil continental lagomorph *Prolagus oeningensis* and three fossil species of insular *Prolagus* displays parallel-fibred primary bone and reticular, radial as well as longitudinal vascularisation. Typical for large mammals, secondary bone in the giant rhinocerotoid *Paraceratherium* sp. from the Late Oligocene of Turkey is represented by dense Haversian bone. The skeletochronological features of *Sinomegaceros yabei*, a large-sized deer from the Pleistocene of Japan closely related to *Megaloceros*, indicate a high growth rate. These examples and the synthesis of existing data show the potential of bone microstructure to reveal essential information on life history evolution. The bone tissue and the skeletochronological data of the sampled island species suggest the presence of various modes of bone histological modification and mammalian life history evolution on islands to depend on factors of island evolution such as island size, distance from mainland, climate, phylogeny, and time of evolution.

Mammalian bone palaeohistology: new data on island forms and a survey

Christian Kolb[1*], Torsten M. Scheyer[1], Kristof Veitschegger[1], Analia M. Forasiepi[2], Eli Amson[1], Alexandra van der Geer[3], Lars W. van den Hoek Ostende[3], Shoji Hayashi[4], Marcelo R. Sánchez-Villagra[1]

[1]*Paläontologisches Institut und Museum der Universität Zürich, Karl Schmid-Strasse 4, CH-8006 Zürich, Switzerland (christian.kolb@pim.uzh.ch, Tel. +41(0)446342269; tscheyer@pim.uzh.ch, Tel.: +41(0)446342322; kristof.veitschegger@pim.uzh.ch, Tel.: +41(0)446342329; eli.amson@pim.uzh.ch, Tel +41(0)446342148; m.sanchez@pim.uzh.ch, Tel. +41(0)446342342)*

[2] *Consejo Nacional de Investigaciones Científicas y Técnicas (CONICET), Instituto Argentino de Nivología, Glaciología y Ciencias Ambientales (IANIGLA), Centro Científico y Tecnológico (CCT), Av. Ruiz Leal s/n° 5500, Mendoza-ciudad, Mendoza, Argentina (acanthodes@gmail.com, Tel. +54(261)5244253)*

[3] *Naturalis Biodiversity Center, P.O. Box 9517, 2300 RA Leiden, The Netherlands (alexandra.vandergeer@naturalis.nl, Tel. +31(0)717517390; lars.vandenhoekostende@naturalis.nl, Tel.* +31(0)715687685*)*

[4] *Osaka Museum of Natural History, Nagai Park 1-23, Higashi-Sumiyoshi-Ku, Osaka, 546-0034, Japan (hayashi@mus-nh.city.osaka.jp)*

*Corresponding author

Abstract

The interest in mammalian palaeohistology has increased dramatically in the last two decades. Starting in 1849 via descriptive approaches, it has been demonstrated that bone tissue and vascularisation types correlate with several biological variables such as ontogenetic stage, growth rate, and ecology. Mammalian bone displays a large variety of bone tissues and vascularisation patterns reaching from lamellar or parallel-fibred to fibrolamellar or woven-fibred bone, depending on taxon and individual age. Here we systematically review the knowledge and methods on cynodont and mammalian bone as well as palaeohistology and discuss potential future research fields and techniques. We present new data on the bone microstructure of two extant marsupial species and of several extinct continental and island placental mammals. Recent marsupials display mainly parallel-fibred primary bone with radial, oblique, but mainly longitudinal vascular canals. Three juvenile specimens of the dwarf island hippopotamid *Hippopotamus minor* from the Late Pleistocene of Cyprus show reticular to plexiform fibrolamellar bone. The island murid *Mikrotia magna* from the Late Miocene of Gargano, Italy displays parallel-fibred primary bone with reticular vascularisation and compact coarse cancellous bone in the central part of the cortex. *Leithia* sp., the dormouse from the Pleistocene of Sicily, is characterised by a primary bone cortex consisting of lamellar bone and low vascularisation. The bone cortex of the fossil continental lagomorph *Prolagus oeningensis* and three fossil species of insular *Prolagus* displays parallel-fibred primary bone and reticular, radial as well as longitudinal vascularisation. Typical for large mammals, secondary bone in the giant rhinocerotoid *Paraceratherium* sp. from the Late Oligocene of Turkey is represented by

dense Haversian bone. The skeletochronological features of *Sinomegaceros yabei*, a large-sized deer from the Pleistocene of Japan closely related to *Megaloceros*, indicate a high growth rate. These examples and the synthesis of existing data show the potential of bone microstructure to reveal essential information on life history evolution. The bone tissue and the skeletochronological data of the sampled island species suggest the presence of various modes of bone histological modification and mammalian life history evolution on islands to depend on factors of island evolution such as island size, distance from mainland, climate, phylogeny, and time of evolution.

Introduction

Histology of fossil bones (e.g. Ricqlès, 1976a; Padian, 2011) provides data to investigate life history variables such as age, sexual maturity, growth patterns, and reproductive cycles. Research on fossil vertebrate hard tissues dates back to the 19th century when it was recognised that bones and teeth are commonly very well preserved at the histological level (Quekett, 1849a; Quekett, 1849b). Since then, several descriptive surveys of different tetrapod taxa, including mammals, were published (e.g. Schaffer, 1890; Enlow & Brown, 1958; Ricqlès, 1976a; Ricqlès, 1976b; Klevezal, 1996; Marin-Moratalla et al., 2014; Prondvai et al., 2014). The study of the microstructure of highly mineralised components such as blood vessel arrangement (de Boef & Larsson, 2007) and tissue types in bones as well as teeth (e.g. Kolb et al., 2015) provides information on growth patterns and remodelling processes of hard tissues in extinct vertebrates (see also Scheyer, Klein & Sander, 2010; Chinsamy-Turan, 2012a; and Padian & Lamm, 2013 for summaries).

Mammals are a well-known group of vertebrates with a well-documented fossil record. However, until recent years and apart from a few seminal papers (Gross, 1934; Enlow & Brown, 1958; Warren, 1963; Klevezal, 1996), mammalian bone histology received little attention by biologists and palaeontologists alike compared to dinosaurs and non-mammalian synapsids (e.g. Horner, Ricqlès & Padian, 1999; Sander et al., 2004; Chinsamy-Turan, 2012a; see also Padian, 2013 for a review on Chinsamy-Turan, 2012a).

The present contribution summarises the main aspects about the current state of knowledge on mammalian palaeohistology without omitting some of the relevant non-mammalian contributions, presents new finds on several extant and extinct species from diverse clades, and discusses perspectives in this field of research. Bone histological traits of extinct island mammals sampled for the present study are described and implications for island evolution are discussed. Literature dealing with pathologies in mammalian bone is omitted since this goes beyond the scope of this synthesis.

Bone tissue types

In synapsids, three main types of bone matrix are distinguished. *Woven-fibred bone* shows highly disorganised collagen fibres of different sizes being loosely and randomly arranged. *Parallel-fibred bone* consists of tightly packed collagen fibrils arranged in parallel. *Lamellar bone* shows the highest spatial organisation. It consists of thin layers (lamellae) of closely packed collagen fibres. Both parallel-fibred and lamellar bone are indicative of relatively low growth rates (Francillon-Vieillot et al., 1990; Huttenlocker , Woodward & Hall, 2013). Bromage et al. (2009) confirmed that lamellar bone is an incremental tissue, with one lamella formed in the species-specific time dependency of the formation of long-period increments

(striae of Retzius) in enamel. The authors showed as well a negative correlation between osteocyte density in bone and body mass and therefore suggested a central autonomic regulatory control mechanism to the coordination of organismal life history and body mass. This demonstrates the relevance of bone histology for understanding physiological mechanisms in extant and extinct vertebrates.

A bone complex composed of a woven-fibred bone matrix in which osteonal lamellar bone infills the space between woven bone and primary vascular canals, is defined as *fibrolamellar bone* (Figs. 1B, 1C, 1E, 1F) (Ricqlès, 1974; Stein & Prondvai, 2013) or fibrolamellar complex (FLC; Ricqlès, 1975; Ricqlès et al., 1991; Margerie, Cubo & Castanet, 2002, Prondvai et al., 2014). According to its vascular orientation, three main types of fibrolamellar bone are distinguished: *Laminar bone* shows an almost uniform circumferential orientation of vascular canals. In case circumferential canals are connected by radial ones forming a dense anastomosing network, the pattern is called *plexiform* (Figs. 1B, 1C, 1E, 1F). An anastomosing network showing random organisation with oblique orientations is defined as reticular. Moreover, a radial arrangement of vascular canals is called *radiating* or *radial bone* (Francillon-Vieillot et al., 1990; Chinsamy-Turan, 2012b; Huttenlocker, Woodward & Hall, 2013).

Amprino identified for the first time a relationship between bone tissue type and growth rate in vertebrates, what is now called “Amprino’s rule” (Amprino, 1947; see also Lee et al., 2013). Stein & Prondvai (2013) found, by investigating longitudinal thin sections of sauropod long bones, that the amount of woven bone in the primary complex has been largely overestimated (e.g., Klein & Sander 2008), questioning former arguments on the biology and life history of sauropod dinosaurs. Similarly, Kolb et al. (2015) showed, via longitudinal thin

sections, that in the giant deer *Megaloceros giganteus* the amount of woven-fibred bone within the fibrolamellar complex (FLC) is easily overestimated as well.

Growth marks and skeletochronology

Different types of growth marks in the bone cortex are distinguished in the osteohistological literature. They are deposited cyclically, usually occurring within lamellar or parallel-fibred bone. All kinds of growth marks indicate a change in growth rate or a complete arrest of growth.

In all groups of mammals thin, semitranslucent to opaque bands, termed lines of arrested growth (LAGs, see also Huttenlocker, Woodward & Hall, 2013), occur (Morris, 1970; Frylestam & Schantz, 1977; Buffrénil, 1982; Chinsamy, Rich & Vickers-Rich, 1998; Klevezal, 1996; Castanet et al., 2004; Köhler et al., 2012). It has repeatedly been confirmed and is now widely accepted that LAGs are deposited annually (e. g. Castanet & Smirina, 1990; Buffrénil & Castanet, 2000; Castanet, 1994; Marangoni et al., 2009; Chinsamy-Turan, 2012b) and independently of metabolic rate and climatic background (Köhler et al., 2012; Huttenlocker, Woodward & Hall, 2013) and therefore they can be used for age estimations, estimates of age at sexual or skeletal maturity, and growth rate analysis.

Castanet et al. (2004) studied LAGs in long bones, mandibles, and tooth cementum (M2 and M3) of captive specimens of known age of the mouse lemur, *Microcebus murinus*. The 43 male and 23 female specimens sampled ranged from juveniles to 11-year-old adults, for which LAG counts and ages correlated best in the tibiae. In individuals older than seven years the correlation decreased, leading to an age underestimation of three to four years and demonstrating limitations of skeletochronology in long bones (see also Klevezal, 1996; Castanet, 2006).

Additionally, animals exposed to an artificially accelerated photoperiodic regimen (a 10-month cycle) show a higher number of LAGs than animals of the same true age in which a yearly photoperiod is maintained. According to that, there is strong evidence that photoperiodicity is an essential factor for the deposition of LAGs rather than environmental factors (see also Woodward, Padian & Lee, 2013).

Köhler et al. (2012) additionally demonstrated that the annual formation of LAGs is present throughout ruminants and that a cyclic arrest of growth in bone is mainly triggered by hormonal cues rather than environmental stresses. By confirming seasonal deposition of LAGs throughout ruminants, the general occurrence of LAGs in homeothermic endotherms has been confirmed, precluding the use of lines of arrested growth as an indicator of ectothermy (Köhler et al., 2012).

Different kinds of processes in the cortex potentially remove parts of the growth record and may erase early LAGs. One of those processes is the substitution of primary bone tissue by secondary bone tissue in areas where resorption previously occurred. Secondary bone can appear as *Haversian bone* (Fig. 1I) consisting of clustered Haversian systems as a response to damage such as microcracks or around the medullary cavity forming endosteal lamellar bone as a response to ontogenetic changes in bone shape, i.e. bone drift (Enlow, 1962).

Several approaches to retrocalculate the lost information have been attempted and there are two ways of retrocalculating missing years. First, in case an appropriate ontogenetic growth series sampling is not available, it is possible to do arithmetic estimates of the missing intervals, done first for dinosaurs (e.g. Sander & Tückmantel, 2003; Horner & Padian, 2004; Erickson et al., 2004). The second approach is the superimposition of thin sections of long bones of different ontogenetic stages as, again done first for dinosaurs (e.g. Horner, Ricqlès & Padian, 2000;

Bybee, Lee & Lamm, 2006; Lee & Werning, 2008; Erickson, 2014; see also Woodward, Padian & Lee, 2013 for more methodological details).

Marin-Moratalla, Jordana & Köhler (2013) were the first to apply the superimposition method to mammals using anteroposterior diameters of successive growth rings in five antelope (*Addax*) femora of different ages. They found that the first LAG in adult specimens fits the second growth cycle of juveniles, indicating that the first LAG is lost by resorption throughout ontogeny. On one hand, this allowed estimates of age at death by counting all the rest lines in the bone cortex and increasing the LAG count by one. On the other hand, it was possible to estimate age at sexual maturity. When an animal becomes mature, this is indicated by the deposition of a narrow layer of avascular lamellar bone, called the *outer circumferential layer* (OCL, Ponton et al., 2004; Figs. 1B, 1C), also referred to as the *external fundamental system* (EFS, *sensu* Horner, Ricqlès & Padian, 1999; see also Woodward, Padian & Lee, 2013). Given that Cormack (1987) uses the term "outer circumferential lamellae" (p. 305), we follow Ponton et al. (2004) in using the term outer circumferential layer (OCL) instead of EFS. Marin-Moratalla, Jordana & Köhler (2013) and Jordana et al. (in press) interpreted the transition from the FLC to the OCL to represent attainment of reproductive maturity in ruminants , since maturity estimates correlated well with individual tooth eruption and wear stages, as well as life history data. Therefore, the authors could show that in ruminants it is possible to determine age at reproductive maturity and death. Maturity estimates based on the occurrence of the OCL in a recent study by Kolb et al. (2015) in extant cervids based on bone microstructure corresponded well with the timing of the attainment of skeletal maturity.

Material and methods

In order to contribute to a more complete picture of mammalian palaeohistology, long bones of the following additional mammalian taxa of which the bone histological characteristics are not or only poorly documented in the literature, including several taxa of extinct insular mammals, were sampled (Table 1): The extant white-eared opossum *Didelphis albiventris* and the thick-tailed opossum *Lutreolina crassicautada*, the giant deer *Megaloceros giganteus* from the Late Pleistocene of Ireland, the Asian giant deer *Sinomegaceros yabei* from the Late Pleistocene of Japan, the extant southern pudu *Pudu* puda, the Cyprus dwarf hippopotamid *Hippopotamus minor* from the Late Pleistocene of Cyprus, the dormouse *Leithia* sp. from the Pleistocene of Sicily, the giant hornless rhinocerotoid *Paraceratherium* sp. from the Late Oligocene of Turkey, the continental pika *Prolagus oeningensis* from the Middle Miocene of La Grive, France, and the Sardinian pika *Prolagus sardus* from the Late Pleistocene. From the Late Miocene of Gargano, Italy, the following material was sampled: The galericine insectivore *Deinogalerix* sp., the giant murid *Mikrotia magna*, as well as the giant pikas *Prolagus apricenicus* and *Prolagus imperialis*. Ontogenetic stages in long bones have been determined by the state of epiphyseal fusion (Habermehl, 1985).

Following standard procedures, bones were coated and impregnated with epoxy resin (Araldite or Technovit) prior to sawing and grinding. Long bones were transversely sectioned at mid-shaft where the growth record is most complete (e.g. Sander & Andrassy 2006; Kolb et al., 2015). Long bones of *Megaloceros giganteus* were also sampled by using a diamond-studded core drill, with sampled cores being subsequently processed (Sander & Andrassy, 2006; Stein & Sander, 2009). Sections were observed in normal transmitted and cross-polarised light using a Leica DM 2500 M compound microscope equipped with Leica DFC 420 C digital camera.

Phylogenies were produced using Mesquite 3.02© (Maddison & Maddison, 2015) and redrawn using Adobe Illustrator CS5©.

Approval information – We thank Naturalis Biodiversity Center, Leiden, the Netherlands, Loïc Costeur (Naturhistorisches Museum Basel, Switzerland), George Lyras (Museum of Paleontology and Geology, University of Athens, Greece), Nigel Monaghan (National Museum of Ireland, Natural History), Hiroyuki Taruno (Osaka Museum of Natural History, Japan), Frank Zachos and Alexander Bibl (Naturhistorisches Museum Wien, Austria), Pierre-Olivier Antoine (Institut des Sciences de l'Evolution-Montpellier, France), and Ebru Albayrak, (MTA Natural History Museum, The General Directorate of Mineral Research and Exploration, Ankara, Turkey) for approving sampling of specimens for histological study.

Mammalian bone histology – works before 1935

The initial contribution on the bone palaeohistology of mammals was performed by Quekett (1849a, 1849b, 1855) as part of comprehensive studies dealing with the bone cortex of not only mammals but also fish, reptiles, and birds. He described mammalian long bone tissue comprising a fossil rhinocerotid and an equid, the fossil giant deer *Megaloceros giganteus*, the fossil proboscidean *Mastodon*, fossil xenarthrans such as *Megatherium*, and humans to show Haversian canals, bony laminae, bone-cells, and canaliculi as well as a the typical three layered composition of cranial bones, ribs, and scapulae displaying a diploe structure within two thin compact layers . Aeby (1878) concentrated on taphonomical aspects and compared bone tissue of reptiles, birds, and mammals. Kiprijanoff (1881) illustrated in a comparative study of fossil material from Russia the bone cortex of the sperm whale (*Physeter macrocephalus*). Schaffer (1890) described the bone tissue of several mammalian taxa, including sirenians from the

Eocene, Oligocene, and Miocene (*Halitherium*), a proboscidean from the Miocene (*Mastodon*), an undetermined fossil cetacean, and artiodactyls (an undetermined artiodactyl referred to an antelope and to *Hippopotamus*, both from the Pliocene). Schaffer also investigated Artiodactyla (*Sus scrofa,Capreolus*), Carnivora (*Ursus spelaeus*), Rodentia (*Arvicola*), as well as undetermined long and skull bones, all from the Pleistocene. Foote (1911a, 1911b) examined in a comprehensive study the femoral bone cortex of extant amphibians, birds, and mammals, including marsupials, rodents, lagomorphs, carnivorans, 'ungulates', and primates. Nopcsa and Heidsieck (1934) studied apart from reptile bones, ribs of sirenians (*Halitherium*). In his comparative work, Gross (1934) studied the bone cortex of the proboscidean *Mammuthus*.

Bone histology of extinct and extant cynodont clades

Non-mammalian cynodonts – Cynodonts represent the last major synapsid lineage to appear in Earth history with mammals as living representatives. Many articles have been published on non-mammalian cynodont histology in recent years (e.g. Ricqlès, 1969; Botha & Chinsamy 2000; Botha & Chinsamy, 2004; Botha & Chinsamy, 2005; Ray, Botha & Chinsamy, 2004; Chinsamy & Abdala, 2008; Botha-Brink, Abdala & Chinsamy, 2012; Chinsamy-Turan, 2012b). Fibrolamellar bone is present to a varying degree in all cynodonts. Considerable variation in vascular density and orientation and the presence/absence of growth marks such as LAGs are evident. When observed within the phylogenetic context, there is an overall increase in bone deposition rate. This is indicated by an increasing prevalence of highly vascularised fibrolamellar bone in phylogenetic later cynodonts (Botha-Brink, Abdala & Chinsamy, 2012). Several factors are discussed to influence the microstructure and therefore being responsible for the aforementioned variability: phylogeny, biomechanics, ontogeny, body size, lifestyle

preferences, and environmental influences (Cubo et al., 2005; Kriloff et al., 2008; Botha-Brink, Abdala & Chinsamy, 2012). Padian (2013) emphasised that the correlation between fibrolamellar bone and high growth rates as well as endothermy is still valid, although fibrolamellar bone is known to occur in rare cases in ectothermic reptiles such as crocodiles and turtles.

Multituberculata and early mammals – Studies on multituberculate (see Fig. 2 for mammalian groups discussed below) and in general stem mammalian histology are scarce. Enlow & Brown (1958) described the section of a mandible of *Ptilodus*. Its cortex consisted of lamellar bone with a central region of indistinct and unorganised lamellae, in which lacunae and cell spaces as well as radial vascular canals were present. Morphological studies have suggested different kinds of locomotion within the group (saltatorial, fossorial, scansorial, and arboreal; Kielan-Jaworowska, Zifelli & Luo, 2004), which might be reflected in the microstructure of the appendicular bones. Chinsamy & Hurum (2006) analysed in a comparative study the bone tissue of long bones and one rib of multituberculates and early mammals. They showed that *Morganucodon* and multituberculates (*Kryptobataar*, *Nemegtbataar*) were characterised by fibrolamellar/woven-fibred bone at early stages of ontogeny and later on by parallel-fibred or lamellar bone. These finds pointed towards relatively high growth rates compared to the late Mesozoic eutherians *Zalambdalestes* and *Barunlestes* with periodic growth pauses as indicated by the occurrence of LAGs. Comparisons of morganucodontid and early mammalian bone microstructure with that of non-mammalian cynodonts, extant monotremes, and placentals indicated significant differences in the rate of osteogenesis in the various groups. The authors concluded multituberculates and Mesozoic eutherians to have had slower growth rates than modern monotremes and placentals and that the sustained, uninterrupted bone formation among multituberculates may have been an adaptive attribute prior to the K−Pg event, but that a flexible

growth strategy implying periodic growth pauses of the early eutherians was more advantageous thereafter.

Monotremata – Monotremes are represented today by three genera (*Ornithorynchus*, *Tachyglossus*, and *Zaglossus*) of specialized skeletal morphology. Their poor fossil record includes material from Australia and South America (Pascual et al., 1992; Musser and Archer 1998). Accordingly, the histology of monotremes has been scarcely studied. Enlow and Brown (1958) were the first to describe sections of long bones and ribs of *Platypus* and *Echidna*. Chinsamy & Hurum (2006) described the femoral bone tissue of *Ornithorhynchus* as being a mixture of woven-fibred bone with lamellar bone deposits. Additionally, large parts of the compacta consisted of compacted coarse cancellous bone. The type of vascularisation and the orientation of the vascular channels varied from simple blood vessels with longitudinal, circular and radial orientations to primary osteons with longitudinal and reticular arrangements. Only isolated secondary osteons were present.

Marsupialia – Despite marsupials being the second most diverse group of living mammals, their bone histology is poorly studied so far. Early contributions are those of Foote (1911a), Enlow & Brown (1958) and Singh (1974) on the marsupial *Didelphis*. Our study of new samples of the white-eared opossum *Didelphis albiventris* and the latrine opossum *Lutreolina crassicaudata* (Table 1) essentially confirms their observations.

The bone cortex of *Didelphis* long bones is characterised by a compacta surrounding the medullary cavity. The bone matrix is dominated by parallel-fibered bone (Figs. 3A-C). Towards the inner part, the amount of woven-fibered bone increases (Fig. 3C). In most specimens remodelling is restricted to isolated secondary osteons as described by Enlow & Brown (1958). In specimen PIMUZ A/V 5278, remodelling is abundant in the central part of the cortex, being

formed by Haversian bone with mainly obliquely oriented and partially irregularly shaped secondary osteons. Inner and outer circumferential layers are present. The inner circumferential layer consists of lamellar bone. The outer circumferential layer is dominated by parallel-fibered bone. The thickness of this layer varies between specimens. Except in one specimen showing one LAG, no LAGs are present in the analysed specimens.. The bone cortex is well vascularised up to the outer part of the cortex (see also Enlow & Brown, 1958), with an irregular pattern, i.e. radial, oblique, but mainly longitudinal primary vascular canals. *Lutreolina* shows a primary bone matrix that is dominated by parallel-fibered bone with simple primary longitudinal and radial to oblique vascular canals (Figs. 3D-F). Remodelled areas are characterised by partially oblique secondary osteons (Fig. 3F). The inner circumferential layer is thin and formed by lamellar bone. The outer circumferential layer is, if present, formed by parallel-fibered bone. LAGs are not developed. The vascularity is less dense than in *Didelphis*. The combination of parallel-fibered bone with low vascularisation suggests slow apposition rates (Chinsamy-Turan, 2012b; Huttenlocker, Woodward & Hall, 2013).

Xenarthra – Early contributions on xenarthran bone histology are Quekett (1849; 1855) and Enlow and Brown (1958). Because dermal armour is an outstanding feature of xenarthrans, several studies focussed on the histology of osteoderms (e.g. Wolf, 2007; Wolf, 2008; Chávez-Aponte et al., 2008; Hill, 2006; Vickaryous & Hall, 2006; Krmpotic et al., 2009; Vickaryous & Sire, 2009; Wolf, Kalthoff & Sander, 2012; Da Costa Pereira et al., 2012). These data shed light on soft tissue structures of extinct xenarthrans, their phylogenetic relationships as well as their functional morphology, which otherwise are not available. The most detailed study up to date dealing with xenarthran long bone histology was performed by Straehl et al., 2013 (but see also Ricqlès, Taquet & Buffrénil, 2009). Straehl and colleagues sampled 67 long bones of 19 genera

and 22 xenarthran species and studied bone microstructure as well as bone compactness trends. Primary bone tissue consists of a mixture of woven, parallel-fibred and lamellar bone. Irregularly shaped vascular canals show longitudinal, reticular or radial orientation. Anteaters are the only sampled taxa showing laminar orientation. Armadillo long bones are characterised by obliquely oriented secondary osteons in transverse sections, reflecting their complex morphology. LAGs are common in xenarthrans although being restricted to the outermost part of the bone cortex in armadillo long bones. Moreover, cingulates (armadillos and closely relative extinct taxa) show lower bone compactness than pilosans (sloths) and an allometric relationship between humeral and femoral compactness. Straehl and colleagues emphasise that remodelling is more developed in larger taxa as indicated by dense Haversian bone in adult specimens and discuss increased loading as a possible cause. Amson et al. (2014) assessed the timing of acquisition of osteosclerosis (increase in bone compactness) and pachyostosis (increase in bone volume) in long bones and ribs of the aquatic sloth *Thalassocnus* from the Neogene of Peru as the main osteohistological modifications of terrestrial tetrapods returning to water. They showed that such modifications can occur during a short geological time span, i.e. *ca* 4 Ma. Furthermore, the strongly remodelled nature of xenarthran bone histology allowed the reassignment of a rib previously ascribed to a sirenian to the aquatic sloth (Amson et al., 2015).

Afrotheria – Early contributions on the bone histology of afrotherians are Aeby (1878) and Schaffer (1890) on sirenians and proboscideans, Nopcsa & Heidsieck (1934) on sirenians, Vanderhoof (1937), Enlow & Brown (1958), Kaiser (1960), Mitchell (1963; 1964) on sirenians and desmostylians, and Ezra & Cook (1959) as well as Cook, Brooks & Ezra-Cohn (1962) on elephantids. Ricqlès & Buffrénil (1995) described pachyosteosclerosis in the sirenian *Hydrodamalis gigas*. Buffrénil et al. (2008; 2010) studied the ribs of 15 extant and extinct

sirenian species representing 13 genera, one desmostylian, and 53 specimens of 42 extant species of terrestrial, aquatic or amphibious mammals. Primary bone tissue in young specimens is constituted by fibrolamellar bone, whereas with increasing age, parallel-fibred bone tissue with longitudinal vascular canals and frequent LAGs is deposited. The authors showed that pachyostosis is subsequently regressed during evolution of the clade. In contrast, only by the end of the Eocene, osteosclerosis was fully developed. It was argued that variable degrees of pachyostosis and osteosclerosis in extinct and extant sirenians were caused by similar heterochronic mechanisms bearing on the timing of osteoblast activity. Hayashi et al. (2013) analysed the histology of long bones, ribs, and vertebrae of four genera of desmostylians (usually considered as tethytherians, but see Cooper et al., 2014) and 108 specimens of extant taxa (ribs: 19 taxa, humeri: 62 taxa, femora: 16 taxa, vertebrae: 11 taxa) with various phylogenetic positions and ecologies by using thin sections and CT-scan data. Primary bone tissue in desmostylians consisted of parallel-fibred bone with multiple LAGs. By comparisons with extant mammals, they found that *Behemetops* and *Palaeoparadoxia* show osteosclerosis, *Ashoroa* pachyosteosclerosis (i.e. a combination of increase in bone volume and compactness), while *Desmostylus* shows an osteoporotic-like pattern (i.e. decrease in bone compactness) instead. Since it is known from extant mammals that bone mass increase provides hydrostatic buoyancy and body trim control suitable for passive swimmers and shallow divers, whereas spongy bones are associated with hydrodynamic buoyancy control in active swimmers, they concluded that all desmostylians achieved an essentially aquatic lifestyle. However, the basal taxa *Behemotops*, *Paleoparadoxia* and *Ashoroa* could be interpreted as shallow water swimmers hovering slowly or walking on the bottom, whereas the derived taxon *Desmostylus* was a more active swimmer.

366 The study has therefore shown that desmostylians are the second mammalian group after
367 cetaceans to show a shift from bone mass increase to decrease during their evolutionary history.
368 As several tethytherian taxa are aquatic, the question of the ancestral lifestyle of the clade
369 was raised. A femur and a humerus of the Eocene proboscidean *Numidotherium* were sampled
370 by Mahboubi et al. (2014). These authors recognised “large medullar cavities” (p. 506), which
371 was considered as suggestive of terrestrial habits. However, the illustrations provided by
372 Mahboubi et al. (2014) show no opened medullary cavity, as trabecular bone occupies most of
373 the cross-sectional area (labelled “medullary bone” by Mahboubi et al., 2014: Fig. 4).
374 Sander & Andrassy (2006) described the bone tissue of *Mammuthus primigenius* long
375 bones as laminar fibrolamellar bone. Due to poor preservation of the fossil bone tissue, the
376 authors have not been able to definitely confirm the occurrence of LAGs. The valuable study of
377 Curtin et al. (2012) dealt with two aspects of bone histology. First, they described for the first
378 time the bone tissue of fifteen bones (femora and tibiae) of eleven specimens of late-term-fetal,
379 neonatal, and young juvenile extant and extinct elephantids representing four species, including
380 the insular dwarf mammoth *Mammuthus exilis* from the Late Pleistocene of Santa Rosa Island of
381 the Californian Channel Islands. The bone tissue they found was predominantly laminar
382 fibrolamellar bone. Remarkable was a distinct change in tissue microstructure marking the
383 boundary between prenatal and postnatal bone deposition, i.e. a higher amount of large
384 longitudinal vascular canals suggesting slightly higher postnatal growth rates. Secondly, besides
385 histological thin sections, Curtin and colleagues employed synchrotron microtomography (SR-
386 µCT) for noninvasively obtaining high-resolution image-“slices”. They showed that, in
387 comparison to histological sectioning, the SR-µCT data lack shrinkage, distortion or loss of
388 tissue, as is usually the case in histological sections. However, they stated that the quality of

389 histological detail observable is by far superior in histological thin sections. The virtual
390 microtomography enabled the authors to rank specimens by ontogenetic stage and quantified
391 vascular patterns. They showed that bones of the Columbian mammoth, *M. columbi* had the
392 thickest and largest number of laminae, whereas the insular dwarf mammoth, *M. exilis*, was
393 characterised by its variability in that regard. The authors concluded that, qualitatively, patterns
394 of early bone growth in elephantids are similar to those of juveniles of other tetrapods, including
395 dinosaurs.

396 *Notoungulata* – Notoungulates are an extinct, largely diverse, endemic group of Cenozoic
397 South American mammals, ecologically similar to current hoofed ungulates. Only four taxa
398 (*Toxodon*, *Nesodon*, *Mesotherium*, and *Paedotherium*) were subject to histological studies
399 (Ricqlès, Taquet & Buffrénil, 2009; Forasiepi et al., 2014; Tomassini et al., 2014) from the more
400 than 150 species recognised in the group. The bone samples were characterised by a well-
401 vascularised compact cortex with mostly longitudinal vascular canals. Few irregularly oriented
402 canals could also be found. Osteocyte lacunae were large and very abundant. Haversian bone
403 was recorded in *Toxodon*, *Nesodon*, and *Mesotherium*. This is a common feature in mammalian
404 bone (Enlow & Brown, 1958), probably caused by increased loading in large-bodied species as
405 discussed by Straehl et al. (2013) for xenarthrans. Areas of primary bone matrix were visible
406 between secondary osteons, which displayed a mostly parallel-fibered to lamellar organisation.
407 Localized areas of woven bone characterised by round osteocyte lacunae were also present. The
408 most external layer of the cortex consisted of parallel-fibred bone with only very few secondary
409 osteons and was in clear contrast to the heavily remodelled inner cortex. The study of Tomassini
410 et al. (2015) on the palaeohistology of hemimandibles of *Paedotherium bonaerense* from the

411 early Pliocene of Argentina discussed the processes affecting fossil remains before and after
412 burial.

413 *Pantodonta* - Pantodonts are an extinct group of mammals that comprised large-bodied,
414 heavily built omnivores and herbivores, from the Paleocene and Eocene of Laurasia. Only one
415 study (Enlow and Brown 1958) examined the bone histology of this group. The rib of the Eocene
416 pantodont *Coryphodon* showed primary lamellar bone with longitudinal vascularisation.

417 *Laurasiatheria – Eulipotyphla* - The comprehensive work of Enlow & Brown (1958)
418 gave the first contribution on eulipotyphlan bone histology. They described the primary bone
419 tissue of a *Talpa* tibia and a *Sorex* mandible as almost completely avascular lamellar bone. A
420 juvenile humerus and radius showed in their outer cortex a "disorganised" (Enlow & Brown,
421 (1958: p. 190) called it, being accompanied by oblique, radial, circumferential or longitudinal
422 simple vascular canals. Klevezal (1996) discussed eulipotyphlan histology by emphasising
423 growth marks (LAGs) in the bone cortex of mandibles and their value for skeletochronology.
424 Meier et al. (2013) studied the bone compactness of humeri of eleven extant and eight fossil
425 talpid species and two non-talpid species. They could not detect any pattern of global
426 compactness related to biomechanical specialization, phylogeny or size and concluded that at
427 this small size the overall morphology of the humerus plays a predominant role in absorbing
428 load. Morris (1970) evaluated the applicability of LAGs in extant hedgehog mandibles and found
429 high correlation between age and LAG count.

430 In the giant galericine "hedgehog" *Deinogalerix* from the palaeoisland of Gargano (Table
431 1), Italy, the bone tissue at the inner layer of femur RGM.178017 and humerus RGM.425360 is
432 characterised by parallel-fibred bone, whereas the outer layer and the trabecular bone is built by
433 lamellar bone (Figs. 4A-C). In the bone cortex, simple longitudinal vascular canals and primary

434 osteons are present. Primary bone tissue is partially replaced by irregularly shaped partly oblique
435 secondary osteons. In the femur corresponding to an adult individual, five LAGs can be
436 distinguished (Fig. 4C) indicating an individual age of minimum five years.

437 *Chiroptera* – Enlow & Brown (1958) described the primary bone tissue in chiropterans as
438 lamellar bone surrounding a non-cancellous medullary cavity. Klevezal (1996) described the
439 presence of LAGs in chiropteran bone tissue. Herdina et al. (2010) described the bone tissue of
440 the baculum of three *Plecotus* species as lamellar bone surrounding a small medullary cavity
441 similar to the arrangement of a Haversian system whereas the ends of the bone consisted of
442 woven-fibred bone.

443 *Perissodactyla* – Enlow & Brown (1958), Sander & Andrassy (2006), Cuijpers (2006),
444 and Hillier & Bell (2007) described long bones and ribs of fossil and extant equids as being
445 primarily plexiform fibrolamellar with longitudinal vascular canals, accompanied by extensive
446 remodelling including the occurrence of dense Haversian bone. Zedda et al. (2008) found a high
447 amount of Haversian tissue in extant horses and cattle. Osteons of the horse were more numerous
448 and composed of a higher number of well-defined lamellae when compared to those of cattle.
449 Diameter, perimeter and area of osteons and Haversian canals were always higher in horses than
450 in cattle and this pattern was related to their different locomotor behaviour. However, Hillier and
451 Bell (2007) found non-significant differences between Haversian canals of horses and cattle.
452 Enlow and Brown (1958) additionally described a stratified, circumferential pattern of vascular
453 canals in a mandible of a Miocene chalicothere (*Moropus*), i.e. laminar fibrolamellar bone tissue
454 *sensu* Francillion-Vieillot et al. (1990). The authors demonstrated an identical pattern of bone
455 tissues and vascular canals in several ribs of fossil tapirs from the Eocene. Sander & Andrassy
456 (2006) described bone tissue of tibiae of Late Pleistocene woolly rhinocerotid (*Coelodonta*

457 *antiquitatis*). They found predominantly laminar fibrolamellar bone as primary bone type besides
458 a high amount of Haversian bone. Ricqlès, Taquet & Buffrénil (2009) described thin sections of
459 several extant and extinct perissodactyls including chalicotheres, describing the distribution of
460 primary and secondary bone as well as vascularisation. Cooper et al. (2014) considered
461 anthracobunids as stem-perissodactyls, and concluded osteosclerosis in limb bones and ribs of
462 anthracobunids to be consistent with the occupation of shallow-water habitats. Martinez-Maza et
463 al. (2014) analysed the bone tissue of humeri, femora, tibiae and metapodials of the equid
464 *Hipparion concudense* from the upper Miocene site of Los Valles de Fuentidueña (Spain) and
465 showed that the number of growth marks is similar among the different limb bones. They
466 distinguished four age groups and determined that *Hipparion concudense* tended to reach
467 skeletal maturity during its third year of life. Martinez-Maza et al. (2014) identified ontogenetic
468 changes in bone structure and growth rate and distinguished three histological stages of ontogeny
469 corresponding to immature, subadult and adult individuals. Nacarino-Meneses, Jordana &
470 Köhler (in press) studied an ontogenetic series of *Equus hemionus* (Asiatic wild ass). They
471 analysed growth marks in femora of different ontogenetic stages. Bone tissue types and vascular
472 canal orientation varied both during ontogeny and within cross-sections. Skeletochronology
473 generally fitted previous age estimates from dental eruption patterns. A wild adult female
474 attained skeletal maturity at the age of four, a wild male at five years of age.

475 A rib of the giant rhinocerotoid *Paraceratherium* sp. (Fig. 1G, Table 1) from the Late
476 Oligocene of Turkey displays dense Haversian bone (Fig. 1I), whereas the bone cortex is heavily
477 recrystallised and does not allow observations on primary bone.

478 *Cetartiodactyla* – Enlow & Brown (1958) gave a comprehensive overview on the bone
479 histology of artiodactyls. The Miocene artiodactyls *Merycoidodon* and *Leptomeryx* showed in

mandibles, maxillas, and ribs a reticular pattern of primary vascularisation next to secondary Haversian tissue. Extant taxa showed essentially plexiform fibrolamellar bone in long bones and reticular bone tissue in skull bones and mandibles. Singh (1974) studied the long bone tissue of a mature specimen of the blue duiker *Cephalophus manticola*, and two perinatal specimens of the Indian sambar *Cervus unicolor* and the reindeer *Rangifer tarandus*. Whereas *Cephalophus* showed primary longitudinal vascularisation, the perinatal cervids revealed a reticular pattern of vascular canals. Plexiform fibrolamellar bone (Figs. 1B, 1C, 1E, 1F) was confirmed as primary bone tissue in artiodactyls in subsequent publications (Klevezal 1996; Horner, Ricqlès & Padian, 1999; Cuijpers, 2006; Sander & Andrassy, 2006; Hillier et al., 2007; Köhler et al., 2012; Marin-Moratalla, Jordana & Köhler, 2013; Kolb et al., 2015). Marin-Moratalla et al. (2014) identified the primary bone tissue in bovids as laminar to plexiform. They studied 51 femora representing 27 ruminant species in order to determine the main intrinsic or extrinsic factors shaping the vascular and cellular network of fibrolamellar bone. Thus, the authors examined the correlation of certain life history traits in bovids, i.e. body mass at birth and adulthood as well as relative age at reproductive maturity. Quantification of vascular orientation and vascular and cell densities revealed that there is no correlation with broad climatic categories or life history. Instead, the authors found correlation with body mass since larger bovids showed more circular canals and lower cell densities than did smaller bovids. Mitchell and Sander (2014) suggested a three front model consisting of an apposition front, a Haversian substitution front, and a resorption front, and applied this model successfully to a humerus of red deer *Cervus elaphus*. They found moderate apposition and remodelling as well as slow resorption in the red deer specimen. Hofmann, Stein & Sander (2014) examined the lamina thickness in bone tissue (LD) in sauropodomorph dinosaurs and 17 mammalian taxa, including artiodactyls and perissodactyls.

503 They found that LD is relatively constrained within the groups and that mean mammalian LD
504 differs significantly from mean sauropodomorph LD. LD in suids was higher than in other
505 mammals. The authors therefore concluded that laminar vascular architecture is most likely
506 determined by a combination of structural, functional as well as vascular supply and
507 physiological causes. Palombo & Zedda (2015) examined a traumatic fracture of a metatarsal of
508 the dwarf deer *Candiacervus ropalophorus* via macroscopic and X-ray analyses. From the size of
509 osseous callus, covering the fracture line and the surface next to the lesion, they concluded that
510 the deer survived several months after the traumatic injury. Furthermore, they concluded that the
511 injured deer only survived for such a long time for the Cretan predator-free insular environment.
512 For the present study, the bone cortex of one small (CKS 110/B), one intermediate (CKS
513 122/B), and one large juvenile (subadult; CKS 117) of the extinct Pleistocene dwarf
514 hippopotamid of Cyprus, *Hippopotamus minor* (also called *Phanourios minor*, see van der Geer
515 et al., 2010) were examined (Table 1). In the juvenile femora the bone tissue is characterised by
516 reticular to plexiform fibrolamellar bone with an endosteal, inner circumferential layer consisting
517 of lamellar bone (Fig. 5). The bone is generally highly vascularised with primary longitudinal
518 vascular canals and primary osteons towards the outer part of the cortex. There are no Haversian
519 systems in the small juvenile (Fig. 5B), although their content increases during ontogeny and is
520 highest in the subadult specimen. Although heavily recrystallized, an adult tibia of
521 *Hippopotamus minor* shows strong remodelling with partially dense Haversian bone occurring
522 from the inner to the outermost part of the cortex. Towards the outer cortex of the subadult femur
523 (Fig. 5D) and typically for large mammals, the amount of parallel-fibred bone within the
524 fibrolamellar complex increases, indicating a decrease in growth rate.

Another taxon sampled for the current study is *Sinomegaceros yabei* (Table 1), which is, as *Megaloceros*, a large-sized megacerine deer. Although a thorough description is prevented by the suboptimal preservation of the specimens, some of their histological features can be given here. The primary bone of the inner cortex is highly vascularised, being formed by fibrolamellar tissue with a mostly plexiform vascularisation. The outer cortex is in turn weakly vascularised. The adult femur OMNH QV-4062 features seven LAGs (Fig. 6), with a 2.57 mm thick second growth zone, which is even greater than the extreme values found in the elk, *Alces* and *Megaloceros* (Kolb et al., 2015), and which indicates, as in the latter taxa, a high growth rate.

Several authors focused on the bone histology of cetaceans and sirenians for their peculiar aquatic lifestyle. Enlow & Brown (1958) described the primary bone tissue of skull bones and vertebrae of the porpoise (*Phocoena phocoena*) as featuring a reticular vascularisation with a high amount of remodelling including the occurrence of dense Haversian bone. Buffrénil and colleagues studied the microstructure of baleen whale bone tissue in several works. They found annually deposited well-defined LAGs in mandibular bone tissue of the common porpoise, *Phocoena phocoena* (Buffrénil, 1982). The humeral bone tissue of the common dolphin (*Delphinus delphis*) shows a cancellous texture without a free medullary cavity and more bone being eroded than deposited during ontogeny indicating an osteoporotic-like process (Buffrénil & Schoevaert, 1988). Buffrénil & Casinos (1995), by using standard microscopic methods, and Zylberberg et al. (1998), by using scanning and transmission electron microscopy, studied the rostrum of the extant Blainville's beaked whale *Mesoplodon densirostris*, demonstrating a high density because of hypermineralised tissue with longitudinal fibres in dense Haversian bone. Buffrénil, Dabin & Zylberberg (2004) demonstrated that the petro-tympanic bone complex in common dolphins consists of reticular to laminar fibrolamellar bone, initially being deposited as

548 loose spongiosa with hypermineralised tissue and without Haversian remodelling. Two Eocene
549 archaeocete taxa were shown to feature pachyostosis with hyperostosis (excessive bone growth)
550 of the periosteal cortex very similar to the condition present in some sirenians (Buffrénil et al.,
551 1990). The comparative study of Gray et al. (2007) analysed the ribs of ten specimens
552 representing five extinct cetacean families from the Eocene as they make their transition from a
553 terrestrial/semiaquatic to an obligate aquatic lifestyle over a 10-million-year period. The authors
554 compared those data to nine genera of extant mammals, amongst them modern dolphins, and
555 found profound changes of microstructure involving a shift in bone function. The mechanisms of
556 osteogenesis were flexible enough to accommodate the shift from a typical terrestrial form to
557 osteosclerosis and pachyosteosclerosis, and then to osteoporosis in the first quarter of the
558 evolutionary history of cetaceans. The limb bones and ribs of *Indohyus*, a taxon closely related to
559 cetaceans, were shown to feature osteosclerosis, and considered as indicative of the use of
560 bottom-walking as swimming mode (Thewissen et al., 2007; Cooper et al., 2012). Ricqlès,
561 Taquet & Buffrénil (2009) published the description of a rediscovered collection of thin sections
562 from the 19th century French palaeontologist Paul Gervais including sections of cetaceans. The
563 most recent study on the bone microstructure of cetaceans is the one of Houssaye, Muizon &
564 Gingerich (2015) analysing the bone microstructure of ribs and vertebrae of 15 archaeocete
565 specimens, i.e. Remingtonocetidae, Protocetidae, and Basilosauridae using microtomography
566 and virtual thin-sectioning (i.e. CT scanning). They found bone mass increase in ribs and femora,
567 whereas vertebrae are essentially spongeous. Humeri changed from compact to spongeous
568 whereas femora in basilosaurids became, for not being involved in locomotion, reduced,
569 displaying strong osteosclerosis. The authors concluded that Remingtonocetidae and
570 Protocetidae were probably shallow water swimmers, whereas basilosaurids, for their osseous

specializations similar to those of modern cetaceans, are considered more active open-sea swimmers.

Creodonta – As it is the case for many other vertebrate taxa, Enlow and Brown (1958) are until today the only workers to have analysed the bone tissue of mammalian predators from the Paleogene and Early Neogene of North America, Africa, and Eurasia, the "creodonts". Bone tissue of mandibles, ribs, and long bones has shown to consist of primary lamellar bone with longitudinal/radial vascularisation and secondary Haversian tissue, in general similar to the bone tissue found in modern carnivorans.

Carnivora – Enlow & Brown (1958) studied the mandible bone tissue of *Ursus* and found primary reticular bone and secondary dense Haversian bone, whereas a rib showed only dense Haversian bone. In the outer part, the bone cortex of *Ursus* consisted of plexiform bone. Chinsamy, Rich & Vickers-Rich (1998) found several LAGs in the zonal bone cortex of the polar bear. Hayashi et al. (2013) reported that the polar bear (*Urusus maritimus*) displays microanatomical features close to those of active swimmers in its limb bones, particularly in the humerus, and intermediate between aquatic and terrestrial taxa in the femur, despite its morphological features, which do not show particular adaptation for swimming. However, *U. maritimus* long bones still displayed a true medullary cavity. The authors suggested that this result, and notably the apparently stronger adaptation of the humerus for an aquatic mode of life, is probably linked to its swimming style because *U. maritimus* uses the forelimbs as the main propulsors during swimming.

Mephitis (skunk), *Procyon* (raccoon), *Mustela* (badger), *Felis* (cat), *Canis* (dog), and *Urocyon* (fox) all possess reticular and radial primary bone (Enlow & Brown 1958). However, the bone cortex of adult specimens in these taxa was dominated by secondary Haversian bone.

The outer cortex of *Canis* was composed of primary plexiform bone tissue. The mongoose (*Herpestes*) showed in its femur primary longitudinal vascularised bone devoid of Haversian remodelling whereas the bone cortex of the American mink (*Neovison vison*) was composed of reticular and Haversian bone.

Singh (1974) found in felids and mustelids lamellar bone with radial to longitudinal vascularisation. Klevezal & Kleinenberg (1969) found annual LAGs in the bone cortex of carnivorans. Several works dealt with the accuracy of LAGs in carnivorans in comparison to dental histology as a tool of age determination: Johnston & Beauregard (1969) (*Vulpes*), Pascale & Delattre (1981) (*Mustela*), King (1991) (*Mustela*), Klevezal (1996) (*Mustela*, *Martes*), Pascal & Castanet (1978) (*Felis*). The outcome was always in favour of dental cementum analysis. Buffrénil & Pascal (1984) concluded that in mink mandibles the deposition of LAGs is not strictly annual by using fluorescein and alizarin labelling.

The long bones of *Valenictus*, a Pliocene walrus (Odobenidae), were described as being osteosclerotic (Deméré, 1994). Nakajima & Endo (2013) and Nakajima, Hirayama & Endo (2014) analysed humeral microanatomy of multiple carnivore taxa including terrestrial, semi-aquatic and fully-aquatic taxa. The authors used CT-scans and found variations of bone organisation in the centre of bone ossification and in the humeral head among carnivorans including different modes of life. Cancellousness in the centre of bone ossification is relatively low in the semiaquatic taxa like the sea otter and is relatively high both in terrestrial taxa like the wolverine and highly aquatic taxa such as the southern elephant seal. Trabeculae in humeral heads are fine and well-organised in terrestrial to semi-aquatic taxa, while those of aquatic ones are rather coarse and randomly oriented.

616 *Euarchontoglires – Rodentia* – Early contributions on rodent bone histology were made
617 by Foote (1911a), Enlow & Brown (1958) as well as Singh (1974). More recent ones are those of
618 Klevezal (1996) on rest lines and age determination, Martiniakova et al. (2005) on rat bone
619 histology, and Garcia-Martinez et al. (2011) on the bone histology of dormice. The bone tissue of
620 rodents mainly consists of lamellar or parallel-fibred bone with reticular, radial or longitudinal
621 vascularisation as primary bone tissue. Development of Haversian systems is rare. Geiger et al.
622 (2013) studied the bone cortex of a femur of the giant caviomorph *Phoberomys pattersoni* from
623 the Miocene of Trinidad, and found it to be composed of lamellar-zonal bone. The specimen
624 sampled showed alternating layers of compacted coarse cancellous bone and parallel-
625 fibered/lamellar primary bone with a reticulum-like structure. The authors reported Haversian
626 tissue to be absent. Montoya (2014) examined the bone microstructure of the recent subterranean
627 rodent *Bathyergus suillus* (Bathyergidae). The author found a thickening of the compacta during
628 ontogeny in contrast to cursorial and bipedal mammals as well as females to display a wide
629 variation of microanatomical parameters, showing resorptive activity already from juvenile
630 ontogenetic stages.

631 The femoral bone cortex of *Mikrotia magna*, a giant insular murine rodent from the Late
632 Miocene former island of Gargano (Italy; Table 1), consists merely of compact bone. The bone
633 matrix of the central part of the cortex is dominated by parallel-fibred bone with reticular
634 vascularisation and compact coarse cancellous bone (Enlow, 1962; Geiger et al., 2013; Montoya,
635 2014) (Figs. 7A-C) including small areas of woven-fibred bone, producing a distinct
636 disorganised pattern (Enlow & Brown, 1958). The disorganised centre of the cortex is
637 additionally pervaded by few mainly irregularly shaped and partially obliquely oriented,
638 secondary osteons. The inner and outer parts of the cortex are formed by lamellar bone with poor

longitudinal but mainly radial vascularisation. The thickness of those parts varies throughout the circumference of the bone cortex and between samples, and is rarely interrupted by thin layers of woven-fibred bone. All the samples display LAGs. In the adult femur RGM.792085, four to five LAGs are counted. Resorption cavities are present close to the medullary cavity.

Thin sections of the femur of the dormouse *Leithia* sp. from the Pleistocene of Sicily (Table 1) are characterised by a compact cortex. The primary bone matrix is formed by lamellar bone pervaded by large and mainly irregularly shaped and partially obliquely oriented secondary osteons (Figs. 7D-F). LAGs are absent in the sampled specimen. Large resorption cavities and small areas of compact coarse cancellous bone occur. The primary vascularisation is weak and limited to only few longitudinal to radial vascular canals.

Lagomorpha – For this study four different species of ochotonids (*Prolagus*) were investigated (Table 1). One mainland form (*Prolagus oeningensis* from La Grive France) and three island forms: The giant species *Prolagus sardus* (Sardinia, Italy) (Fig. 8A) and *P. imperialis* along with *P. apricenicus*, both from Gargano, Italy. Generally, the bone cortex of the femur and the humerus of *Prolagus* is compact. It is characterised by a bone matrix changing from fibrolamellar to parallel-fibered into lamellar bone from the central cortex towards the OCL (Figs. 8B-F). An endosteal lamellar layer is present. In most specimens the fibrolamellar or parallel-fibred bone is partly pervaded by mainly irregularly shaped and partially obliquely oriented secondary osteons, producing the “subendosteal layer of Haversian-like bone” *sensu* Pazzaglia et al. (2015: Fig. 6B). The primary bone cortex is in general weakly vascularised. Within the primary fibrolamellar and parallel-fibred bone, primary and simple longitudinal vascular canals as well as radial and reticular vascular canals occur and are arranged in an irregular manner. LAGs indicating minimum ages are present in some adult specimens. *Prolagus*

662 *oeningensis* (Figs. 8B, 8C) gives a maximum count of three LAGs, *Prolagus apricenicus* a
663 maximum count of two LAGs, and *Prolagus imperialis* as well as *Prolagus sardus* each gives a
664 maximum count of five LAGs (Figs. 8D-F). Juvenile femora of *Prolagus oeningensis* (PIMUZ
665 A/V 4532) and *Prolagus sardus* (NMB Ty. 4974; Fig. 8E) as well as a juvenile humerus of
666 *Prolagus imperialis* (RGM.792102) are in the inner and central part of the cortex characterised
667 by longitudinal, radial, and reticular vascularised fibrolamellar bone with a high amount of
668 woven bone. Towards the bone surface, the amount of parallel-fibered bone is increasing and the
669 vascularisation changes into longitudinal simple and primary vascular canals. Primary bone
670 tissue is pervaded by mainly obliquely oriented and partially irregularly shaped secondary
671 osteons in the inner and central part of the cortex already in juvenile specimens. Our
672 observations on lagomorph bone histology essentially agree with Foote's (1911a) and Enlow &
673 Brown's (1958) observations on lagomorphs. The same is the case for the study of Pazzaglia et
674 al. (2015), who studied rabbit (*Oryctolagus cuniculus*) femora of different ontogenetic stages via
675 micro CT-scanning. However, what they call laminar respectively plexiform bone tissue is not in
676 agreement with the nomenclature of Francillon-Vieillot et al. (1990) used by us, i.e. longitudinal,
677 radial, and reticular vascularisation. Moncunill-Solé et al. (in press) provided mass estimates of
678 350 g for the extinct continental *Prolagus* cf. *calpensis*, and 280 – 600 g for *Prolagus*
679 *apricenicus* based on femoral measurements. Bone histological analysis suggested a longevity
680 for *Prolagus apricenicus* of at least seven years (five years more than in our sample of *P.*
681 *apricenicus*). Moncunill-Solé et al. (in press) suggested, based on the predictions by the body
682 mass inferred, a move to the slow end of the fast-slow continuum (maturing later and fewer
683 offspring) in *Prolagus apricenicus*.

Primates - Again, Enlow & Brown (1958) were the first to describe the bone tissue of extinct primates by sampling a mandible of the fossil Paleocene *Plesiolestes* and long bones of modern primates. The authors described primary bone tissue formed by lamellar bone. Vascularisation was mainly characterised by longitudinal primary vascular canals. Remodelling was partially abundant and the organisation of Haversian bone was in some areas of the bone cortex even dense. Those observations have been confirmed by the comparative studies of Cuijpers (2006) and Hillier & Bell (2007) as well as the conceptual ones of Bromage et al. (2009; see also above) and Castanet (2006; see also above). Castanet et al. (2004; see also above) found the inner and thicker part of the bone cortex of *Microcebus* long bones to be formed by parallel-fibred bone containing primary blood vessels and scarce primary osteons. In contrast, the outer part of the cortex is not vascularised. Crowder & Stout (2012) have compiled a book regarding the current utilisation of histological analysis of bones and teeth within the field of anthropology, including the biology and growth of bone, histomorphological analysis, and age determination. There is extensive literature on hominoids, especially on bone pathologies in *Homo sapiens*, and in order not to go beyond the scope of this work, we cite here only some examples of publications in this area. Martinez-Maza, Rosas & García-Vargas (2006) and Martinez-Maza et al. (2011) analysed bone surfaces under the reflected light and scanning electron microscope in order to decipher modelling and remodelling patterns in extant hominine facial skeletons and mandibles as well as in Neanderthal mandibles, explaining specific morphological traits. Schultz and Schmidt-Schultz (2014) examined fossil human bone and reviewed the methods and techniques of light microscopy, scanning electron microscopy, and advantages of polarisation microscopy for palaeoanthropology. In this context it is noteworthy that estimation of individual age in anthropology is carried out by mainly two methods (Schultz

& Schmidt-Schultz, 2014): (1) the histomorphometric method (HMM) and (2) the histomorphologic method (HML). The HMM method is applied mainly to long bones (e.g. Kerley, 1965; Drusini, 1987) and is based upon the frequencies of osteons (Haversian systems), fragmented osteons (interstitial lamellae), non-Haversian canals, and the percentage of the external circumferential lamellae. The HML method is based upon the morphology (presence, size, shape, development) of external and internal circumferential lamellae, osteons, fragmented osteons, and non-Haversian canals (e.g. Schultz, 1997). Skinner et al. (2015) studied pattern of trabeculae distribution of metacarpals in *Australopithecus africanus* and Pleistocene hominins. They found a 'human-like' pattern, considered as consistent with tool use. Ryan & Shaw (2015) quantified the proximal femur trabecular bone structure using micro-CT data from 31 extant primate taxa (229 individuals) and four distinct archaeological human populations (59 individuals) representing sedentary agriculturalists and mobile foragers. Trabecular bone variables indicate that the forager populations had significantly higher bone volume fraction, thicker trabeculae, and lower relative bone surface area compared with the two agriculturalist groups. The authors did not find any significant differences between agriculturalist and forager populations for trabecular spacing, number, or degree of anisotropy. Ryan & Shaw concluded in revealing a correspondence between human behaviour and bone structure in the proximal femur, indicating that more highly mobile human populations have trabecular bone structure similar to what would be expected for wild non-human primates of the same body mass, thus emphasising the importance of physical activity and exercise for bone health and the attenuation of age-related bone loss.

Selected contributions on mammalian histology

In the following part, selected contributions on mammalian histology are separately discussed, since they deserve a more detailed evaluation in our view because they address special aspects and/or applications of palaeohistological work. Enlow & Brown's (1958) outstanding comparative work on mammalian bone histology is not further mentioned in this section, since it is repeatedly discussed above.

Klevezal & Kleinenberg (1969) were the first to recognise the presence and importance of rest lines in the bone cortex of mammals for skeletochronological studies (see also Chinsamy-Turan, 2005). In their work, which was originally published in Russian in 1967, they found that in mammals, unlike the zonal bone forming in reptiles, the recording part including LAGs is the outer or periosteal zone (see also above). Klevezal (1996) found that not in every mammalian taxon rest lines are formed from the first year of life. Therefore she suggested a variable correction factor for different mammalian taxa, and concluded that the best structures for recording growth and age are dentine and especially cementum (Klevezal, 1996). In her detailed and comprehensive study of recording structures in mammals, she found that the growth rate of a particular structure can change according to the growth rate of the whole organism and that seasonal changes of growth intensity of an animal as a whole determine the formation of growth layers. Klevezal (1996) argued that changes in humidity, not temperature, may play a role as seasonal factor in growth.

Dumont et al. (2013) documented the microstructure of vertebral centra using 2D histomorphometric analyses of vertebral centra of 98 therian mammal species that cover the main size ranges and locomotor adaptations known in therian taxa. The authors extracted eleven variables relative to the development and geometry of trabecular networks from CT scan mid-sagittal sections. Random taxon reshuffling and squared change parsimony indicated a

753 phylogenetic signal in most of the variables. Furthermore, based on those variables, it was
754 possible to discriminate three categories of locomotion among the sampled taxa: a) terrestrial +
755 flying + digging + amphibious forms, b) coastal oscillatory aquatic taxa, and c) pelagic
756 oscillatory aquatic forms represented by oceanic cetaceans. Dumont and colleagues concluded
757 that, when specific size increases, the length of trabecular networks, as well as trabecular
758 proliferation, increase with positive allometry. They found that, by using six structural variables,
759 locomotion mode can be predicted with a 97.4% success rate for terrestrial forms, 66.7% for
760 coastal oscillatory, and 81.3% for pelagic oscillatory.

761 Sander & Andrassy (2006) described the occurrence of LAGs in 21 long bones (mainly
762 tibiae and metatarsals) of herbivorous mammals from the Late Pleistocene of Germany
763 comprising the extinct giant deer *Megaloceros giganteus*, the red deer *Cervus elaphus*, the
764 reindeer *Rangifer tarandus*, the extinct bovids *Bos primigenius* and *Bison priscus*, the equid
765 *Equus* sp., the extinct rhinocerotid *Coelodonta antiquitatis*, and the extinct elephantid
766 *Mammuthus primigenius*. All samples showed fibrolamellar bone and a varying degree of
767 remodelling and most of the long bones displayed LAGs. Because of the frequent find of LAGs
768 in endothermic animals the authors questioned the argument that LAGs in dinosaur bone indicate
769 ectothermy.

770 Köhler & Moyà-Solà (2009) examined the long-bone histology of *Myotragus*, a Plio-
771 Pleistocene bovid from the Balearic Islands. It revealed lamellar-zonal tissue throughout the
772 cortex, a trait exclusive to ectothermic reptiles. According to Köhler and colleagues, *Myotragus*
773 grew unlike any other mammal but similar to crocodiles at slow and flexible rates, ceased growth
774 periodically, and attained somatic maturity late by 12 years. The authors concluded that this

775 developmental pattern indicates that *Myotragus*, much like extant reptiles, synchronized its
776 metabolic requirements with fluctuating resource levels.

777 Kolb et al. (2015) performed a histological analysis of long bones and teeth representing
778 eleven extinct and extant cervid taxa, amongst them the dwarf island morphotypes of
779 *Candiacervus* from the Late Pleistocene of Crete and the giant deer *Megaloceros giganteus*, both
780 in a clade together with fallow deer (*Dama dama*) among extant species. Bone tissue types
781 observed have been similar, indicating a comparable mode of growth across the eight species
782 examined, with long bones mainly possessing primary plexiform fibrolamellar bone (Figs. 1B,
783 1C, 1E, 1F). Dwarf *Candiacervus* have been characterised by low growth rates, *Megaloceros* by
784 high rates, and the lowest recorded rates were those of the Miocene small stem cervid
785 *Procervulus praelucidus*. It can be noted that *Sinomegaceros yabei*, sampled for the present
786 study, features a very thick second growth zone, which suggests a high growth rate, comparable
787 to that of the closely related *Megaloceros*. Skeletal maturity estimates (see also above) indicated
788 late attainment in sampled *Candiacervus* and *Procervulus*. Tooth cementum analysis of first
789 molars of two senile *Megaloceros giganteus* specimens revealed ages of 16 and 19 years whereas
790 two old dwarf *Candiacervus* specimens gave ages of 12 and 18 years. Kolb et al. (2015)
791 concluded that the bone histological condition found in *Candiacervus* has features in common
792 with that of *Myotragus* (Köhler & Moyà-Solà, 2009), but is achieved with a lesser modification
793 of bone tissue and suggested various modes of life history and size evolution among island
794 mammals. Amson et al. (in press) examined further ‘stem-cervid’ bone histology in describing
795 that of other Miocene taxa, *Dicrocerus elegans* and *Euprox* sp. With their inclusion in the dataset
796 of Kolb et al. (2015), they estimated ancestral growth rates among cervids, and studied their
797 correlation with body size. The skeletochronology of *Dicrocerus* and *Euprox* suggested

relatively high and intermediate growth rates respectively for their body sizes, differing from the condition of *Procervulus*, and hence documenting diversity in the life history traits of Miocene cervids.

Discussion on bone histology of island mammals

Three juvenile specimens of the dwarf island hippopotamid *Hippopotamus minor* from the Late Pleistocene of Cyprus show reticular to plexiform fibrolamellar bone, which does not indicate an island-specific pattern of bone growth or life history but a mode of growth similar to continental hippopotamid relatives instead. The bone cortex of the dormouse *Leithia* sp. from the Pleistocene of Sicily is characterised by lamellar bone and low vascularisation. *Mikrotia magna*, the giant island rodent from the Late Miocene of Gargano, Italy shows in the central part of the cortex parallel-fibred bone with reticular vascularisation and compact coarse cancellous bone, additionally pervaded by few mainly irregularly shaped and partially obliquely oriented, secondary osteons, whereas the inner and outer parts of the cortex are formed by lamellar bone. Three fossil species of insular giant *Prolagus* and the fossil continental lagomorph *Prolagus oeningensis* exhibit in their bone cortex mainly parallel-fibred bone and reticular, radial as well as longitudinal vascularisation thus indicating similarity of bone histological arrangements in continental and island species of rodents and lagomorphs.

The highest minimum age found in *Prolagus sardus* and *P. imperialis* of five years are well within the known longevities of extant ochotonids such as *Ochotona princeps* (seven years in captivity) and *O. hyperborean* (9.4 years in captivity) (Tacutu et al., 2013). A minimal individual age deduced from growth marks in the bone tissue of *Deinogalerix* specimen RGM 178017 lies also well within the known longevities for extant erinaceids such as *Erinaceus*

europaeus (11.7 years in captivity), *E. concolor* (seven years in captivity), and *E. amurensis* (9.4 years in captivity) whereas longevity data for extant galericines are not yet available (Tacutu et al., 2013).

The insular dwarf bovid *Myotragus balearicus* from Majorca showed an important decrease in bone growth rate and an evolution towards a slow life history, i.e. delayed maturity and long lifespan (Köhler and Moyà-Solà, 2009; Köhler, 2010; Jordana & Köhler, 2011; Jordana et al., 2012; Moncunill-Solé et al., in press; but see Raia, Barbera & Conte (2003). The authors suggested these findings to be trends for island mammals in agreement with McArthur & Wilson (1967), as well as life history theory (Stearns, 1992) and that the degree of these modifications depends on multiple factors as island size, distance from mainland, climate, phylogeny, time of evolution and others (see also Moncunill-Solé et al., 2014). *Myotragus* dwelt on Majora for 5.2 Ma and therefore underwent an exceptionally long time of evolution (van der Geer et al., 2010) and resource limitation (Köhler & Moyà-Solà, 2009). A similarly high degree of bone histological and life history modification as described by Köhler & Moyà-Solà (2009) for *Myotragus* in comparison to continental artiodactyls was not recorded for the insular mammals *Deinogalerix* sp., *Hippopotamus minor*, *Leithia* sp., *Mikrotia magna*, and several species of *Prolagus* in comparison to their mainland relatives.

A lower degree of modification in bone tissue and life history could be related to shorter persistence times and different island size (Lomolino et al., 2012; Lomolino et al., 2013; Kolb et al., 2015)., in line with Austad & Fischer (1991), McNab (1994; 2002; 2010), Raia, Barbera & Conte (2003), Curtin et al. (2012), and Kolb et al. (2015).

Conclusions

844 A large variety of bone tissues and vascularisation patterns is encountered in mammalian
845 bone reaching from lamellar or parallel-fibred to fibrolamellar or woven-fibred bone, largely
846 depending on taxon and individual age. A plexiform to laminar organisation of vascular canals
847 within fibrolamellar bone is typically found in taxa containing large-bodied species such as non-
848 mammalian cynodonts, laurasiatherians, and afrotherians. The deposition of Haversian systems
849 throughout ontogeny of synapsids is common, only in rodents their content is usually low. Table
850 2 gives a summary on general patterns of bone histological features encountered in major
851 synapsid clades.
852 We suggest the presence of various modes of bone histological modification and
853 mammalian life history evolution on islands depending on factors of island evolution such as
854 island size, distance from mainland, climate, phylogeny, and time of evolution. Further bone
855 histological comparisons and sampling of more specimens as well as species of fossil insular
856 endemics and their mainland relatives within an ontogenetic framework would contribute
857 significantly to the knowledge of the ecology of past island ecosystems.
858
859 **Future research fields**
860 *New technologies* - 3D reconstructions attained by virtual image analysis gain increasing
861 importance for palaeontological research at the anatomical, microanatomical, and even
862 histological levels (Sanchez et al., 2012; Clément & Geffard-Kuriyama, 2010; Curtin et al.,
863 2012; see also Ricqlès, 2011). The potential advantages of virtual imaging as a method are
864 obvious: First, specimens do not have to be damaged for invasive sampling. Second, a third
865 dimension, usually gained by time consuming serial sectioning or preparation of orthogonally
866 oriented thin sections, is easily available. Third, virtual imaging techniques allow continuous

867 "zooming" from the histological to the micro- and macronatomical levels of structural
868 organisation. High resolution synchrotron virtual histology provides new 3D insights into the
869 submicron-scale histology of fossil and extant bones. This is based on the development of new
870 data acquisition strategies, pink-beam configurations, and improved processing tools (Sanchez et
871 al., 2012). Nevertheless, for the high resolution optical properties of a polarisation microscope
872 and their applications for identification and analysis of bone microstructure and as well for the
873 comparatively low amount of financial resources needed, traditional thin sections are far from
874 being completely replaced by virtual imaging techniques. Moreover, new statistical methods
875 allow extraction of phylogenetic signals from bone microstructure and of high specimen numbers
876 (Laurin, 2004; Laurin, Girondot & Loth, 2004; Cubo et al., 2008). High performance computers
877 additionally sustain attainment of ecological, biomechanical, and phylogenetic signals (Cubo et
878 al., 2005; Cubo et al., 2008; Laurin, Girondot & Loth, 2004; Laurin et al., 2004; Ricqlès & Cubo,
879 2010; Hayashi et al., 2013) taking into account the variability of bone tissues produced by
880 multiple factors. The creation of histological databases will soon be necessary due to an
881 increasing number of palaeohistological publications and growing collections of thin sections
882 (Ricqlès, Castanet & Francillon-Vieillot, 2004; Ricqlès, Taquet & Buffrénil, 2009; Bromage,
883 2006; Kriloff et al., 2008; Scheyer, 2009-2015; Canoville & Laurin, 2010; O'Leary &
884 Kaufmann, 2012).

885 *Extant vertebrate biology* - Actualistic models are essential for the interpretation of fossil
886 hard tissues in every sense, no matter if developmental and life historical, histophysiological,
887 morphological, ecological, or systematic. Living animals present the basis for inferring
888 palaeobiological conclusions and this has already been done in several bone histological works

(e.g. Canoville & Laurin, 2010; Köhler et al., 2012, Marin-Moratalla, Jordana & Köhler, 2013; Marin-Moratalla et al., 2014; Kolb et al. 2015).

Especially in regard of deciphering life history signals, the actualistic approach is and will become increasingly fundamental (e.g. Köhler & Moyà-Solà, 2009; Köhler et al., 2012; Marin-Moratalla, Jordana & Köhler, 2013; Marin-Moratalla et al., 2014; Kolb et al., 2015). Life history variables such as annual growth rate, somatic/sexual maturity, and longevity and their signal in bone microstructure help to understand the palaeobiology not only of fossil mammals but tetrapods in general. It is possible using bone histology to quantify growth rates and vascularisation or cellular density in mammals as a relative proxy for growth rate (Curtin et al., 2012; Kolb et al., 2015; Marin-Moratalla, Jordana & Köhler, 2013), whereby the existing literature on the paleobiology of dinosaurs has been used as a starting point. However, not every methodological approach used for dinosaurs is applicable or relevant for mammals (e.g. Erickson, Curry Rogers & Yerby, 2001; Griebeler, Klein & Sander, 2013; Kolb et al., 2015). No one stated it better than Armand de Ricqlès: „The possibilities of using bone histology of extant vertebrates for various fundamental or applied research, whether on life history traits, ecology, or microevolution, are simply boundless.“ (Ricqlès, 2011).

Acknowledgments

Alexandra Wegmann and Fiona Straehl are thanked for help with bone histological preparation, and Madeleine Geiger for fruitful discussions (all Palaeontological Institute of the University of Zurich, Switzerland). Likewise, we thank Xavier Jordana and P. Martin Sander for their thorough and critical reviews, which greatly helped to improve the manuscript.

References

Aeby C. 1878. Das histologische Verhalten fossilen Knochen- und Zahngewebes. *Archiv für Mikroskopische Anatomie* 15:371-382.

Agustí J, and Antón M. 2002. *Mammoths, sabertooths and hominids*. New York: Columbia University Press.

Amprino R. 1947. La structure du tissu osseux envisagee comme l'expression de différences dans la vitesse de l'accroissement. *Archives de Biologie* 58:315-330.

Amson E, Muizon C de, Laurin M, Argot C, and Buffrénil V de. 2014. Gradual adaptation of bone structure to aquatic lifestyle in extinct sloths from Peru. *Proceedings of the Royal Society B* 281:1-6.

Amson E, Muizon C de, Domning DP, Argot C, and Buffrénil V de. 2015. Bone histology as a clue for resolving the puzzle of a dugong rib in the Pisco Formation, Peru. *Journal of Vertebrate Paleontology*: e922981.

Amson E, Kolb C, Scheyer TM, and Sánchez-Villagra MR. in press. Growth and life history of middle Miocene deer (Mammalia, Cervidae) based on bone histology. *Comptes Rendus Palevol* in press.

Austad SN, and Fischer KE. 1991. Mammalian aging, metabolism, and ecology: Evidence from the bats and marsupials. *Journal of Gerontology* 46:B47-53.

Boef M de, and Larsson HCE. 2007. Bone microstructure: quantifying bone vascular orientation. *Canadian Journal of Zoology* 85:63-70.

Botha J, and Chinsamy A. 2000. Growth patterns deduced from the bone histology of the cynodonts *Diademodon* and *Cynognathus*. *Journal of Vertebrate Paleontology* 20:705-711.

Botha J, and Chinsamy A. 2004. Growth and life habits of the Triassic cynodont *Trirachodon*, inferred from bone histology. *Acta Palaeontologica Polonica* 49:619-627.

Botha J, and Chinsamy A. 2005. Growth patterns of *Thrinaxodon liorhinus*, a non-mammalian cynodont from the Lower Triassic of South Africa. *Palaeontology* 48:385-394.

Botha-Brink J, Abdala F, and Chinsamy A. 2012. The radiation and osteohistology of nonmammaliaform cynodonts. In: Chinsamy-Turan A, ed. *Forerunners of mammals: radiation, histology, biology*. Bloomington: Indiana University Press, 223-246.

Bromage TG. 2006. Donald H. Enlow Digital Image Library. *Available at http://www.nyu.edu/dental/enlow/* (accessed 13 May 2015).

943 Bromage TG, Lacruz RS, Hogg R, Goldman HM, McFarlin SC, Warshaw J, Dirks W, Perez-
944 Ochoa A, Smolyar I, Enlow DH, and Boyde A. 2009. Lamellar bone is an incremental tissue
945 reconciling enamel rhythms, body size, and organismal life history. *Calcified Tissue*
946 *International* 84:388-404.

947 Buffrénil V de. 1982. Données préliminaires sur la présence de lignes d'arret de croissance
948 périostiques dans la mandibule du marsouin commun, *Phocoena phocoena* (L.), et leur
949 utilisation comme indicateur de I'age. *Canadian Journal of Zoology* 60:2557-2567.

950 Buffrénil V de, Astibia H, Pereda Suberbiola X, and Berreteaga A. 2008. Variation in bone
951 histology of middle Eocene sirenians from western Europe. *Geodiversitas* 30:425-432.

952 Buffrénil V de, Canoville A, D'Anastasio R, and Domning DP. 2010. Evolution of sirenian
953 pachyosteosclerosis, a model-case for the study of bone structure in aquatic tetrapods. *Journal of*
954 *Mammalian Evolution* 17:101–120.

955 Buffrénil V de, and Casinos A. 1995. Observations histologiques sur le rostre de *Mesoplodon*
956 *densirostris* (Mammalia, Cetacea, Ziphiidae): le tissu osseux le plus dense connu. *Annales des*
957 *Sciences Naturelles, Zoologie, Paris, 13e Série* 16:21-36.

958 Buffrénil V de, and Castanet J. 2000. Reptiles age estimation by skeletochronology in the Nile
959 Monitor (*Varanus niloticus*), a highly exploited species. *Journal of Herpetology* 34:414-424.

960 Buffrénil V de, Dabin W, and Zylberberg L. 2004. Histology and growth of the cetacean petro-
961 tympanic bone complex. *Journal of Zoology* 262:371-381.

962 Buffrénil V de, and Pascal B. 1984. Croissance et morphogenèse postnatales de la mandibule du
963 vison (*Mustela vison*, Schreiber): données sur la dynamique et l'interprétation fonctionnelle des
964 dépots osseux mandibulaires. *Canadian Journal of Zoology* 62:2026-2037.

965 Buffrénil V de, Ricqlès Ad, Ray CE, and Domning DP. 1990. Bone histology of the ribs of the
966 archaeocetes (Mammalia: Cetacea). *Journal of Vertebrate Paleontology* 10:455-466.

967 Buffrénil V de, and Schoevaert D. 1988. On how the periosteal bone of the delphinid humerus
968 becomes cancellous: ontogeny of a histological specialization. *Journal of Morphology* 198:149-
969 164.

970 Bybee PJ, Lee AH, and Lamm ET. 2006. Sizing the Jurassic theropod dinosaur *Allosaurus*:
971 assessing growth strategy and evolution of ontogenetic scaling of limbs. *Journal of*
972 *Morphology* 267:347-359.

973 Canoville A, and Laurin M. 2010. Evolution of humeral microanatomy and lifestyle in amniotes,
974 and some comments on palaeobiological inferences. *Biological Journal of the Linnean*
975 *Society* 100:384-406.

976 Castanet J. 1994. Age estimation and longevity in reptiles. *Gerontology* 40:174-192.

977 Castanet J. 2006. Time recording in bone microstructures of endothermic animals; functional
978 relationships. *Comptes Rendus Palevol* 5:629-636.

979 Castanet J, Croci S, Aujard F, Perret M, Cubo J, and de Margerie E. 2004. Lines of arrested
980 growth in bone and age estimation in a small primate: *Microcebus murinus*. *Journal of*
981 *Zoology* 263:31-39.

982 Castanet J, and Smirina EM. 1990. Introduction to the skeletochronological method in
983 amphibians and reptiles. *Annales des sciences naturelles, Zoologie* 11:191-196.

984 Chávez-Aponte EO, Alfonzo-Hernández I, Finol HJ, Barrios N. CE, Boada-Sucre A, and
985 Carrillo-Briceño JD. 2008. Histologia y ultraestructura de los osteodermos fosiles de *Glyptodon*
986 *clavipes* y *Holmesina* sp. (Xenarthra: Cingulata). *Interciencia* 33:616-619.

987 Chinsamy A, and Abdala F. 2008. Palaeobiological implications of the bone microstructure of
988 South American traversodontids (Therapsida: Cynodontia). *South African Journal of*
989 *Science* 104:225-230.

990 Chinsamy A, and Hurum JH. 2006. Bone microstructure and growth patterns of early
991 mammals. *Acta Palaeontologica Polonica* 51:325-338.

992 Chinsamy A, Rich T, and Vickers-Rich P. 1998. Polar dinosaur bone histology. *Journal of*
993 *Vertebrate Paleontology* 18:385-390.

994 Chinsamy-Turan A. 2005. *The microstructure of dinosaur bone: Deciphering biology with fine*
995 *scale techniques*. Baltimore: Johns Hopkins University Press.

996 Chinsamy-Turan A. 2012a. Forerunners of mammals: radiation, histology, biology. Life of the
997 past. Bloomington: Indiana University Press. p 352.

998 Chinsamy-Turan A. 2012b. Microstructure of bones and teeth of nonmammalian therapsids. In:
999 Chinsamy-Turan A, ed. *Forerunners of mammals: radiation, histology, biology*. Bloomington:
1000 Indiana University Press, 65-88.

1001 Clément G, and Geffard-Kuriyama D. 2010. Imaging and 3D in palaeontology and
1002 palaeoanthropology. *Comptes Rendus Palevol* 9:259–264.

1003 Cook SF, Brooks ST, and Ezra-Cohn HE. 1962. Histological studies on fossil bone. *Journal of*
1004 *Paleontology* 36:483-494.

1005 Cooper LN, Seiffert ER, Clementz M, Madar SI, Bajpai S, Hussain ST, and Thewissen JGM.
1006 2014. Anthracobunids from the middle eocene of India and pakistan are stem
1007 perissodactyls. *PloS one* 9:e109232.

1008 Cooper LN, Thewissen JGM, S. Bajpai S, and Tiwari BN. 2012. Postcranial morphology and
1009 locomotion of the Eocene raoellid *Indohyus* (Artiodactyla: Mammalia). *Historical*
1010 *Biology* 24:279-310.

1011 Cormack D. H. 1987. *Ham's histology*. Philadelphia: J. B. Lippincott Company.

1012 Crowder C, and Stout S. 2012. *Bone histology: an anthropological perspective*. Boca Raton:
1013 CRC Press.

1014 Cubo J, Legendre P, Ricqlès A de, Montes L, Margerie E de, Castanet J, and Desdevise Y. 2008.
1015 Phylogenetic, functional and structural components of variation in bone growth rate in
1016 amniots. *Evolution and Development* 10:217-227.

1017 Cubo J, Ponton F, Laurin M, Margerie E de, and Castanet J. 2005. Phylogenetic signal in bone
1018 microstructure of sauropsids. *Systematic Biology* 54:562–574.

1019 Cuijpers A. 2006. Histological identification of bone fragments in archaeology: telling humans
1020 apart from horses and cattle. *International Journal of Osteoarchaeology* 16 465–480.

1021 Curtin AJ, Macdowell AA, Schaible EG, and Roth L. 2012. Noninvasive histological
1022 comparison of bone growth patterns among fossil and extant neonatal elephantids using
1023 synchrotron radiation X-ray microtomography. *Journal of Vertebrate Paleontology* 32:939-955.

1024 Da Costa Pereira PVLG, Victer GD, Porpino KDO, and Bergqvist LP. 2012. Osteoderm
1025 histology of Late Pleistocene cingulates from the intertropical region of Brazil. *Acta*
1026 *Palaeontologica Polonica* 59:543-552.

1027 Deméré TA. 1994. Two new species of fossil walruses (Pinnipedia: Odobenidae) from the upper
1028 Pliocene San Diego Formation, California. *Proceedings of the San Diego Society of Natural*
1029 *History* 29:77-98.

1030 Drusini AZ. 1987. Refinement of two methods for the histomorphometric determination of age
1031 in human bone. *Zeitschrift für Morphologie und Anthropologie* 77:167-176.

1032 Dumont M, Laurin M, Jacques F, Pellé E, Dabin W, and Buffrénil V de. 2013. Inner architecture
1033 of vertebral centra in terrestrial and aquatic mammals: a two-dimensional comparative
1034 study. *Journal of Morphology* 274:570-584.

1035 Enlow DH. 1962. A study of the postnatal growth and remodeling of bone. *American Journal of*
1036 *Anatomy* 110:79-101.

1037 Enlow DH, and Brown SO. 1958. A comparative histological study of fossil and recent bone
1038 tissues. Part III. *Texas Journal of science* 10:187-230.

1039 Erickson GM. 2014. On dinosaur growth. *Annual Review of Earth and Planetary*
1040 *Sciences* 42:675-697.

1041 Erickson GM, Curry Rogers K, and Yerby SA. 2001. Dinosaurian growth patterns and rapid
1042 avian growth rates. *Nature* 412:429-433.

1043 Erickson GM, Makovicky PJ, Currie PJ, Norell MA, Yerby SA, and Brochu CA. 2004.
1044 Gigantism and comparative life-history parameters of tyrannosaurid dinosaurs. *Nature* 430:772-
1045 775.

1046 Ezra HC, and Cook SF. 1959. Histology of mammoth bone. *Science* 129 465–466.

1047 Forasiepi AM, Cerdeño E, Bond M, Schmidt GI, Naipauer M, Straehl FR, Martinelli AG,
1048 Garrido AC, Schmitz MD, and Crowley JL. 2014. New toxodontid (Notoungulata) from the
1049 Early Miocene of Mendoza, Argentina. *Paläontologische Zeitschrift* DOI 10.1007/s12542-014-
1050 0233-5.

1051 Foote JS. 1911a. The comparative histology of femoral bones. *Transactions of the American*
1052 *Microscopical Society* 30:87-140.

1053 Foote JS. 1911b. Preliminary Notice *Transactions of the American Microscopical Society*
1054 30:326-327.

1055 Francillon-Vieillot H, Buffrénil V de, Castanet J, Géraudie J, Meunier FJ, Sire JY, and Ricqlès A
1056 de. 1990. Microstructure and mineralization of vertebrate skeletal tissues. In: Carter JG, editor.
1057 Skeletal Biomineralization: Patterns, Processes and Evolutionary Trends. New York: Van
1058 Nostrand Reinhold. p 471–530.

1059 Frylestam B, and von Schantz T. 1977. Age determination of European hares based on periosteal
1060 growth lines. *Mammal Review* 7:151-154.

1061 Garcia-Martinez R, Marin-Moratalla N, Jordana X, and Köhler M. 2011. The ontogeny of bone
1062 growth in two species of dormice: Reconstructing life history traits. *Comptes Rendus*
1063 *Palevol* 10:489-498.

1064 Geiger M, Wilson LAB, Costeur L, Sánchez R, and Sánchez-Villagra MR. 2013. Diversity and
1065 body size in giant caviomorphs (Rodentia) from the Northern Neotropics—study of femoral
1066 variation. *Journal of Vertebrate Paleontology* 33:1449-1456.

1067 Gray NM, Kainec K, Madar S, Tomko L, and Wolfe S. 2007. Sink or Swim? Bone density as a
1068 mechanism for buoyancy control in early cetaceans. *Anatomical Record* 290:638-653.

1069 Griebeler EM, Klein N, and Sander PM. 2013. Aging, maturation and growth of
1070 sauropodomorph dinosaurs as deduced from growth curves using long bone histological data: an
1071 assessment of methodological constraints and solutions. *PloS one* 8: e67012.

1072 Gross W. 1934. Die Typen des mikroskopischen Knochenbaues bei fossilen Stegocephalen und
1073 Reptilien. *Zeitschrift für Anatomie und Enwicklungsgeschichte* 103:731-764.

1074 Habermehl K-H. 1985. *Altersbestimmung bei Wild- und Pelztieren - Möglichkeiten und*
1075 *Methoden - Ein praktischer Leitfaden für Jäger, Biologen und Tierärzte*. Hamburg, Berlin:
1076 Verlag Paul Parey.

1077 Hayashi S, Houssaye A, Nakajima Y, Chiba K, Ando T, Sawamura H, Inuzuka N, Kaneko N,
1078 and Osaki T. 2013. Bone inner structure suggests increasing aquatic adaptations in Desmostylia
1079 (Mammalia, Afrotheria). *PloS one* 8:e59146.

1080 Herdina AN, Herzig-Straschil B, Hilgers H, Metscher BD, and Plenk HJ. 2010.
1081 Histomorphology of the penis bone (baculum) in the gray long-eared bat *Pleocotus*
1082 *austriacus* (Chiroptera, Vespertilionidae). *The Anatomical Record* 293:1248–1258.

1083 Hill RV. 2006. Comparative anatomy and histology of xenarthran osteoderms. *Journal of*
1084 *Morphology* 267:1441-1460.

1085 Hillier ML, and Bell LS. 2007. Differentiating human bone from animal bone: A review of
1086 histological methods. *Journal of Forensic Sciences* 52:249−263.

1087 Hofmann R, Stein K, and Sander PM. 2014. Constraints on the lamina density of laminar bone
1088 architecture of large-bodied dinosaurs and mammals. *Acta Palaeontologica Polonica* 59 287-
1089 294.

1090 Horner JR, Ricqlès A de, and Padian K. 1999. Variation in dinosaur skeletochronology
1091 indicators: implications for age assessment and physiology. *Paleobiology* 25:295-304.

1092 Horner JR, Ricqlès A de, and Padian K. 2000. Long bone histology of the hadrosaurid
1093 dinosaur *Maiasaura peeblesorum*: growth dynamics and physiology based on an ontogenetic
1094 series of skeletal elements. *Journal of Vertebrate Paleontology* 20:115-129.

1095 Horner JR, and Padian K. 2004. Age and growth dynamics of *Tyrannosaurus rex*. *Proceedings of*
1096 *the Royal Society of London B* 271:1875-1880.

1097 Houssaye A, P. T, Muizon C de, and Gingerich PD. 2015. Transition of Eocene whales from
1098 land to sea: evidence from bone microstructure. *PloS one* 10:e0118409.

1099 Huttenlocker AK, Woodward HN, and Hall BK. 2013. The biology of bone. In: Padian K, and
1100 Lamm E-T, eds. *Histology of fossil tetrapods - Advancing methods, analysis and interpretation*.
1101 Berkeley, Los Angeles, London: University of California Press, 13-34.

1102 Johnston DH, and Beauregard M. 1969. Rabies epidemiology in Ontario. *Bulletin of the Wildlife*
1103 *Disease Association* 5:357-370.

1104 Jordana X, and Köhler M. 2011. Enamel microstructure in the fossil bovid *Myotragus balearicus*
1105 (Majorca, Spain): implications for life-history evolution of dwarf mammals in insular
1106 ecosystems. *Palaeogeography, Palaeoclimatology, Palaeoecology* 300:59-66.

1107 Jordana X, Marín-Moratalla N, DeMiguel D, Kaiser TM, and Köhler M. 2012. Evidence of
1108 correlated evolution of hypsodonty and exceptional longevity in endemic insular mammals.
1109 *Proceedings of the Royal Society of London B: Biological Sciences* 279:3339-3346.

1110 Jordana X, Marín-Moratalla N, Moncunill-Solè B, Nacarino-Meneses C, and Köhler M. in press.
1111 Ontogenetic changes in the histological features of zonal bone tissue of ruminants: a quantitative
1112 approach. *Comptes Rendus Palevol*.

1113 Kaiser HE. 1960. Untersuchungen zur vergleichenden Osteologie der fossilen und rezenten
1114 Pachyostosen. *Palaeontographica Abteilung A* 114:113-196.

1115 Kerley ER. 1965. The microscopic determination of age in human bone. *American Journal of*
1116 *Physical Anthropology* 23:149–163.

1117 Kielan−Jaworowska Z, Cifelli RL, and Luo XZ. 2004. *Mammals from the age of dinosaurs:*
1118 *origins, evolution, and structure*. New York: Columbia University Press.

1119 King CM. 1991. A review of age determination methods for the stoat *Mustela erminea*. *Mammal*
1120 *Review* 21:31-49.

1121 Kiprijanoff W. 1881. Studien über die fossilien Reptilien Russlands. I. Theil. Gattung
1122 *Ichthyosaurus* König. *Mémoires de l'Académie des Sciences de St-Pétersbourg, VIIe Série Tome*
1123 *XXVIII* 8:1-103.

1124 Klein N, and Sander PM. 2008. Ontogenetic stages in the long bone histology of sauropod
1125 dinosaurs. *Paleobiology* 34:247-263.

1126 Klevezal GA. 1996. *Recording structures of mammals. Determination of age and reconstruction*
1127 *of life history*. Rotterdam/Brookfield: A.A.Balkema.

1128 Klevezal GA, and Kleinenberg SE. 1969. *Age determination of mammals from annual layers in*
1129 *teeth and bones*. Jerusalem: Israel Program of Scientific Translations.

1130 Köhler M. 2010. Fast or slow? The evolution of life history traits associated with insular
1131 dwarfing. In: Pérez-Mellado V, and Ramon C, editors. p 261-280.

1132 Köhler M, Marín-Moratalla N, Jordana X, and Aanes R. 2012. Seasonal bone growth and
1133 physiology in endotherms shed light on dinosaur physiology. *Nature* 487:358-361.

1134 Köhler M, and Moyà-Solà S. 2009. Physiological and life history strategies of a fossil large
1135 mammal in a resource-limited environment. *Proceedings of the National Academy of Sciences of*
1136 *the United States of America* 106:20354-20358.

1137 Kolb C, Scheyer TM, Lister AM, Azorit C, de Vos J, Schlingemann MAJ, Rössner GE,
1138 Monaghan NT, and Sánchez-Villagra MR. 2015. Growth in fossil and extant deer and
1139 implications for body size and life history evolution. *BMC Evolutionary Biology* 15:1-15.

1140 Kriloff A, Germain D, Canoville A, Vincent P, Sache M, and Laurin M. 2008. Evolution of bone
1141 microanatomy of the tetrapod tibia and its use in palaeobiological inference. *Journal of*
1142 *Evolutionary Biology* 21:807-826.

1143 Krmpotic CM, Ciancio MR, Barbeito CG, Mario RC, and Carlini AA. 2009. Osteoderm
1144 morphology in recent and fossil euphractine xenarthrans. *Acta Zoologica* 90:339-351.

1145 Laurin M. 2004. The evolution of body size. Cope's rule and the origin of amniotes. *Systematic*
1146 *Biology* 53:594-622.

1147 Laurin M, Girondot M, and Loth M-M. 2004. The evolution of long bone microanatomy and
1148 lifestyle in lissamphibians. *Palaeobiology* 30:589-613.

1149 Lee AH, Huttenlocker AK, Padian K, and Woodward HN. 2013. Analysis of growth rates. In:
1150 Padian K, and Lamm E-T, eds. *Bone histology of fossil tetrapods*. Berkeley: University of
1151 California Press, 217-251.

1152 Lee AH, and Werning S. 2008. Sexual maturity in growing dinosaurs does not fit reptilian
1153 growth models. *Proceedings of the National Academy of Sciences of the United States of*
1154 *America* 105:582-587.

1155 Lomolino MV, Sax DF, Palombo MR, and van der Geer AA. 2012. Of mice and mammoths:
1156 evaluations of causal explanations for body size evolution in insular mammals. *Journal of*
1157 *Biogeography* 39:842-854.

1158 Lomolino MV, van der Geer AA, Lyras GA, Palombo MR, Sax DF, and Rozzi R. 2013. Of mice
1159 and mammoths: generality and antiquity of the island rule. *Journal of Biogeography* 40:1427-
1160 1439.

1161 Luo XZ. 2011. Developmental Patterns in Mesozoic Evolution of Mammal Ears. *Annual Review*
1162 *of Ecology, Evolution, and Systematics* 42:355-380

1163 Luo ZX, and Wible JR. 2005. A Late Jurassic digging mammal and early mammalian
1164 diversification. *Science* 308:103-107.

1165 MacArthur RH, and Wilson EO. 1967. *The theory of island biogeography*. Princeton: Princeton
1166 University Press.

1167 Maddison WP, and Maddison DR. 2015. Mesquite: a modular system for evolutionary analysis.
1168 Version 3.02. *Available at http://mesquiteproject.org.*

1169 Mahboubi S, Bocherens H, Scheffler M, Benammi M, and Jaeger JJ. 2014. Was the Early
1170 Eocene proboscidean *Numidotherium koholense* semi-aquatic or terrestrial? Evidence from
1171 stable isotopes and bone histology. *Comptes Rendus Palevol* 13:501–509.

1172 Marangoni F, Schaefer E, Cajade R, and Tejedo M. 2009. Growth mark formation and
1173 chronology of two neotropical anuran species. *Journal of Herpetology* 43:546-550.

1174 Margerie E de, Cubo J, and Castanet J. 2002. Bone typology and growth rate: Testing and
1175 quantifying 'Amprino's rule' in the mallard (*Anas platyrhynchus*). *Comptes Rendus*
1176 *Biologies* 325:221-230.

1177 Marín-Moratalla N, Cubo J, Jordana X, Moncunill-Solè B, and Köhler M. 2014. Correlation of
1178 quantitative bone histology data with life history and climate: a phylogenetic
1179 approach. *Biological Journal of the Linnean Society* 112:678-687.

1180 Marín-Moratalla N, Jordana X, and Köhler M. 2013. Bone histology as an approach to providing
1181 data on certain key life history traits in mammals: Implications for conservation
1182 biology. *Mammalian Biology* 78:422-429.

1183 Martínez-Maza C, Rosas A, and García-Vargas S. 2006. Bone paleohistology and human
1184 evolution. *Journal of Anthropological Sciences* 84:33-52.

1185 Martinez-Maza C, Rosas A, Garcia-Vargas S, Estalrrich A, and de la Rasilla M. 2011. Bone
1186 remodelling in Neanderthal mandibles from the El Sidron site (Asturias, Spain). *Biology*
1187 *Letters* 7:593e596.

1188 Martinez-Maza C, Alberdi MT, Nieto-Diaz M, and Prado JL. 2014. Life history traits of the
1189 Miocene *Hipparion concudense* (Spain) inferred from bone histological structure. *Plosone*
1190 9:e103708.

1191 Martiniaková M, Grosskopf B, Vondráková M, Omelka R, and Fabiš M. 2005. Observation of
1192 the microstructure of rat cortical bone tissue. *Scripta Medica* 78:45-50.

1193 McNab B. 1994. Resource use and the survival of land and freshwater vertebrates on oceanic
1194 islands. *The American Naturalist* 144:643-660.

1195 McNab BK. 2002. Minimizing energy expenditure facilitates vertebrate persistence on oceanic
1196 islands. *Ecological Letters* 5:693-704.

1197 McNab BK. 2010. Geographic and temporal correlations of mammalian size reconsidered: a
1198 resource rule. *Oecologia* 164:13-23.

1199 Meier PS, Bickelmann C, Scheyer, Koyabu D, and Sánchez-Villagra MR. 2013. Evolution of
1200 bone compactness in extant and extinct moles (Talpidae): exploring humeral microstructure in
1201 small fossorial mammals. *BMC Evolutionary Biology* 13:55.

1202 Meredith RW, Janecka J, Gatesy J, Ryder OA, Fisher CA, Teeling EC, Goodbla A, Eizirik E,
1203 Simão TLL, Stadler T, Rabosky DL, Honeycutt RL, Flynn JJ, Ingram CM, Steiner C, Williams
1204 TL, Robinson TJ, Burk-Herrick A, Westerman M, Ayoub NA, Springer MS, and Murphy WJ.

2011. Impacts of the Cretaceous terrestrial revolution and KPg extinction on mammal diversification. *Science* 334:521-524.

Mitchell EDJ. 1963. Brachydont desmostylian from Miocene of San Clemente Island, California. *Bulletin of the Southern California Academy of Science* 62:192-201.

Mitchell EDJ. 1964. Pachyostosis in desmostylids. *The Geological Society of America Special Paper* 76:214.

Mitchell J, and Sander PM. 2014. The three-front model: a developmental explanation of long bone diaphyseal histology of Sauropoda. *Biological Journal of the Linnean Society* 112:765–781.

Moncunill-Solé B, Jordana X, Marín-Moratalla N, Moyà-Solà S, and Köhler M. 2014. How large are the extinct giant insular rodents? New body mass estimations from teeth and bones. *Integrative Zoology* 9:197-212.

Moncunill-Solé B, Orlandi-Oliverasa G, Jordana X, Rook L, and Köhler M. in press. First approach of the life history of *Prolagus apricenicus* (Ochotonidae, Lagomorpha) from Terre Rosse sites (Gargano, Italy) using body mass estimation and paleohistological analysis. *Comptes Rendus Palevol*.

Montoya GA. 2014. Bone microstructure of the subterranean rodent *Bathyergus suillus* (Rodentia: Bathyergidae) Master's thesis. University of Cape Town – South Africa.

Morris P. 1970. A method for determining absolute age in the hedgehog. *Journal of Zoology* 161:277-281.

Musser AM, and Archer M. 1998. New information about the skull and dentary of the Miocene *Platypus obdurodon dicksoni*, and a discussion of ornithorhynchid relationships. *Philosophical Transactions of the Royal Society of London B* 353:1063-1079.

Nacarino-Meneses C, Jordana X, and Köhler M. in press. First approach to bone histology and skeletochronology of *Equus hemionus*. *Comptes Rendus Palevol*.

Nopcsa F von, and Heidsieck E. 1934. Über eine pachyostotische Rippe aus der Kreide Rügens. *Acta Zoologica* 15:431-455.

O'Leary MA, Bloch JI, Flynn JJ, Gaudin TJ, Giallombardo A, Giannini NP, Goldberg SL, Kraatz BP, Luo Z-X, Meng J, Ni X, Novacek MJ, Perini FA, Randall ZS, Rougier GW, Sargis EJ, Silcox MT, Simmons NB, Spaulding M, Velazco PM, Weksler M, Wible JR, and Cirranello AL. 2013. The Placental Mammal Ancestor and the Post-K-Pg Radiation of Placentals. *Science* 339:662-667.

O'Leary MA, and Kaufman SG. 2012. MorphoBank 3.0: web application for morphological phylogenetics and taxonomy. *Available at http://www.morphobank.org* (accessed 6 May 2015).

1239 Padian K. 2011. Vertebrate palaeohistology then and now: A retrospective in the light of the
1240 contributions of Armand de Ricqles. *Comptes Rendus Palevol* 10:303-309.

1241 Padian K. 2013. Book review: forerunners of mammals: radiation, histology, biology. *Journal of*
1242 *Vertebrate Paleontology* 33:1250-1251.

1243 Padian K, and Lamm E-T. 2013. Bone histology of tetrapods. Berkeley, Los Angeles: University
1244 of California Press. p 285.

1245 Palombo MR, and Zedda M. in press. Surviving in a predator-free environment: hints from a
1246 bone remodelling process in a dwarf Pleistocene deer from Crete. *Comptes Rendus*
1247 *Palevol*.Pascal M, and Castanet J. 1978. Méthodes de la détermination de l'age chez le chat haret
1248 des iles Kerguelen. *Terre et Vie* 32:529-554.

1249 Pascal M, and Delattre P. 1981. Comparaison des différentes méthodes de la détermination de
1250 l'age individuel chez le vison (*Mustela vison* Schreber). *Canadian Journal of Zoology* 59:202-
1251 211.

1252 Pascual R, Archer M, Jaureguizar EO, Prado JL, Godthelp H, and Hand SJ. 1992. First discovery
1253 of monotremes in South America. *Nature* 356:704 - 706.

1254 Pazzaglia UE, Sibilia V, Congiu T, Pagani F, Ravanelli M, and Zarattini G. 2015. Setup of a
1255 bone aging experimental model in the rabbit comparing changes in cortical and trabecular bone:
1256 morphological and morphometric study in the femur. *Journal of Morphology*.

1257 Ponton F, Elzanowski A, Castanet J, Chinsamy A, Margerie E de, Ricqlès A de, and Cubo J.
1258 2004. Variation of the outer circumferential layer in the limb bones of birds. *Acta*
1259 *Ornithologica* 39:21-24.

1260 Prondvai E, Stein KHW, Ricqlès A de, and Cubo J. 2014. Development-based revision of bone
1261 tissue classification: the importance of semantics for science. *Biological Journal of the Linnean*
1262 *Society* 112:799-816.

1263 Quekett JT. 1849a. On the intimate structure of bone as composing the skeleton in the four great
1264 classes of animals, viz., mammals, birds, reptiles, and fishes, with some remarks on the great
1265 value of the knowledge of such structure in determining the affinities of minute fragments of
1266 organic remains. *Transactions of the Microscopical Society of London* 2:46-58.

1267 Quekett JT. 1849b. Additional observations on the intimate structure of bone. *Transactions of the*
1268 *Microscopical Society of London* 2:59-64.

1269 Quekett JT. 1855. *Descriptive and illustrated catalogue of the histological series contained in*
1270 *the museum of the Royal College of Surgeons of England. Volume II. Structure of the skeleton of*
1271 *vertebrate animals*. London: Taylor and Francis.

1272 Raia P, Barbera C, and Conte M. 2003. The fast life of a dwarfed giant. *Evolutionary*
1273 *Ecology* 17:293-312.

1274 Ray S, Botha J, and Chinsamy A. 2004. Bone histology and growth patterns of some
1275 nonmammalian therapsids. *Journal of Vertebrate Paleontology* 24:634-648.

1276 Ricqlès A de. 1969. Recherches palèohistologiques sur les os longs des tetrapodes. II.- Quelques
1277 observations sur la structure des os longs des thériodontes. *Annales de Paléontologie* 55:1-52.

1278 Ricqlès A de. 1974. Evolution of endothermy: histological evidence. *Evolutionary Theory* 1:51-
1279 80.

1280 Ricqlès A de. 1975. Recherches paléohistologiques sur les os longs des tétrapodes VII. - Sur la
1281 classification, la signification fonctionnelle et l'histoire des tissus oseux des tétrapodes. Première
1282 partie, structures. *Annales de paléontologie 61, 51-129* 61:51-129.

1283 Ricqlès A de. 1976a. On bone histology of fossil and living reptiles, with comments on its
1284 functional and evolutionary significance. In: Bellairs A, and Cox CB, eds. *Morphology and*
1285 *Biology of Reptiles*. London and New York: Academic Press, 123-150.

1286 Ricqlès A de. 1976b. Recherches paléohistologiques sur les os longs des tétrapodes. VII. - Sur la
1287 classification, la signification fonctionnelle et l'histoire des tissus osseux des tétrapodes.
1288 Deuxième partie. Fonctions: considérations fonctionnelles et physiologiques. *Annales de*
1289 *Paléontologie* 62:71-126.

1290 Ricqlès A de, and Buffrénil V de. 1995. Sur la présence de pachyostéosclerosis chez la rhytine
1291 de Steller (*Rhytina* (*Hydrodamalis*) *gigas*), sirénian rézent éteint. *Annales des Sciences*
1292 *Naturelles, Zoologie, Paris, 13e Série* 16:47-53.

1293 Ricqlès A de, Castanet J, and Francillon-Vieillot H. 2004. The "message" of bone tissue in
1294 Palaeoherpetology. *Italian Journal of Zoology*:3-12.

1295 Ricqlès A de, and Cubo J. 2010. Le problème de la causalité complexe aux sources de la relation
1296 structuro-fonctionnelle : 1/généralités, 2/l'exemple du tissu osseux. In: Gayon J, and Ricqlès Ad,
1297 eds. *Les Fonctions : des organismes aux artefacts*. Paris: PUF, 179-188.

1298 Ricqlès A de, Meunier FJ, Castanet J, and Francillon-Vieillot H. 1991. Comparative
1299 microstructure of bone. In: Hall BK, ed. *Bone Volume 3: Bone matrix and bone specific*
1300 *products*. Boca Raton: CRC Press, 1-78.

1301 Ricqlès A de, Taquet P, and Buffrénil V de. 2009. "Rediscovery" of Paul Gervais'
1302 paleohistological collection. *Geodiversitas* 31:943-971.

1303 Ricqlès A de. 2011. Vertebrate palaeohistology: past and future. *Comptes Rendus*
1304 *Palevol* 10:509–515.

1305 Ryan TM, and Shaw CN. 2015. Gracility of the modern *Homo sapiens* skeleton is the result of
1306 decreased biomechanical loading. *Proceedings of the National Academy of Sciences of the*
1307 *United States of America* 112:372-377.

1308 Sanchez S, Ahlberg P, Trinajstic K, Mirone A, and Tafforeau P. 2012. Three dimensional
1309 synchrotron virtual paleohistology: a new insight into the world of fossil bone
1310 microstructures. *Microscopy and Microanalysis* 18:1095-1105.

1311 Sander PM, and Andrassy P. 2006. Lines of arrested growth and long bone histology in
1312 Pleistocene large mammals from Germany: What do they tell us about dinosaur
1313 physiology? *Palaeontographica Abteilung A* 277:143-159.

1314 Sander PM, Klein N, Buffetaut E, Cuny G, Suteethorn V, and Le Loeuff J. 2004. Adaptive
1315 radiation in sauropod dinosaurs: bone histology indicates rapid evolution of giant body size
1316 through acceleration. *Organisms, Diversity & Evolution* 4:165-173.

1317 Sander PM, and Tückmantel C. 2003. Bone lamina thickness, bone apposition rates, and age
1318 estimates in sauropod humeri and femora. *Paläontologische Zeitschrift* 77:161-172.

1319 Schaffer J. 1890. Über den feineren Bau fossiler Knochen. *Sitzungsberichte der Kaiserlichen*
1320 *Akademie der Wissenschaften* Mathematisch-Naturwissenschaftliche Classe XCVIII. Band.
1321 Hefte I bis X. Abtheilung III:319-382.

1322 Scheyer TM. 2009-2015. Palaeohistology. In: Sánchez-Villagra MR, editor. Developmental -
1323 Palaeontology net. Zurich: Palaeontological Institute of the University of Zurich. *Available at*
1324 *http://www.developmental-palaeontology.net/palaeohistology/index.php* (accessed 1 June 2015).

1325 Scheyer TM, Klein N, and Sander PM. 2010. Developmental palaeontology of Reptilia as
1326 revealed by histological studies. *Seminars in Cell & Developmental Biology* 21:462-470.

1327 Schultz M. 1997. Microscopic investigation of excavated skeletal remains: a contribution to
1328 paleopathology and forensic medicine. In: Haglund WD, and Sorg MH, eds. *Forensic taphonomy*
1329 *The postmortem fate of human remains*. Boca Raton/New York/London/Tokyo: CRC Press, 201-
1330 222.

1331 Schultz M, and Schmidt-Schultz TH. 2014. Microscopic research on fossil human bone. In:
1332 Henke W, and Tattersall I, eds. *Handbook of paleoanthropology*. 2nd ed. Heidelberg/New York:
1333 Springer, 983-998.

1334 Singh IJ, Tonna EA, and Gandel CP. 1974. A comparative histological study of mammalian
1335 bone. *Journal of Morphology* 144:421-438.

1336 Skinner MM, Stephens NB, Tsegai ZJ, Foote AC, Nguyen NH, Gross T, Pahr DH, Hublin J-J,
1337 and Kivell TL. 2015. Human-like hand use in *Australopithecus africanus*. *Science* 347:395–399.

1338 Stearns SC. 1992. *The evolution of life histories*. Oxford: Oxford University Press.

1339 Stein K, and Prondvai E. 2013. Rethinking the nature of fibrolamellar bone: an integrative
1340 biological revision of sauropod plexiform bone formation. *Biological Reviews*:1-24.

1341 Stein K, and Sander M. 2009. Histological core drilling: a less destructive method for studying
1342 bone histology. First Annual Fossil Preparation and Collections Symposium. Petrified Forest
1343 National Park: Petrified Forest. p 69-80.

1344 Straehl FR, Scheyer TM, Forasiepi AM, MacPhee RD, and Sánchez-Villagra MR. 2013.
1345 Evolutionary patterns of bone histology and bone compactness in xenarthran mammal long
1346 bones. *Plosone* 8:e69275.

1347 Tacutu R, Craig T, Budovsky A, Wuttke D, Lehmann G, Taranukha D, Costa J, Fraifeld VE, and
1348 de Magalhaes JP. 2013. Human Ageing Genomic Resources: Integrated databases and tools for
1349 the biology and genetics of ageing. *Nucleic Acids Research* 41:D1027-D1033.

1350 Thewissen JGM, Cooper LN, Clementz MT, Bajpai S, and Tiwari BN. 2007. Whales originated
1351 from aquatic artiodactyls in the Eocene epoch of India. *Nature* 450:1190-1194.

1352 Tomassini RL, Montalvo CI, Manera T, and Visconti G. 2014. Mineralogy, geochemistry, and
1353 paleohistology of pliocene mammals from the Monte Hermoso Formation (Argentina).
1354 *Paedotherium bonaerense* (Notoungulata, Hegetotheriidae) as a case study. *Ameghiniana*
1355 51:385-395.

1356 van der Geer A, Lyras G, de Vos J, and Dermitzakis M. 2010. *Evolution of island mammals.*
1357 *Adaptation and extinction of placental mammals on islands*. Sussex: Wiley-Blackwell.

1358 Vanderhoof VL. 1937. A study of the Miocene sirenian *Desmostylus*. *University of California*
1359 *Publications in the Geological Sciences* 24:169-262.

1360 Vickaryous MK, and Hall BK. 2006. Osteoderm morphology and development in the nine-
1361 banded armadillo, *Dasypus novemcinctus* (Mammalia, Xenarthra, Cingulata). *Journal of*
1362 *Morphology* 267:1273-1283.

1363 Vickaryous MK, and Sire JY. 2009. The integumentary skeleton of tetrapods: origin, evolution,
1364 and development. *Journal of Anatomy* 214:441-464.

1365 Warren JW. 1963. Growth zones in the skeleton of recent and fossil vertebrates PhD. University
1366 of California.

1367 Wolf D. 2007. Osteoderm histology of extinct and recent Cingulata and Phyllophaga (Xenarthra,
1368 Mammalia): implications for systematics and biomechanical adaptation. *Hallesches Jahrbuch für*
1369 *Geowissenschaften* Beiheft 23:145-151.

1370 Wolf D. 2008. Osteoderm histology of the Cingulata (Xenarthra, Mammalia): implications for
1371 systematics. *Journal of Vertebrate Paleontology* 28:161A.

1372 Wolf D, Kalthoff DC, and Martin Sander PM. 2012. Osteoderm histology of the Pampatheriidae
1373 (Cingulata, Xenarthra, Mammalia): implications for systematics, osteoderm growth, and
1374 biomechanical adaptation. *Journal of Morphology* 273:388-404.

1375 Woodward HN, Padian K, and Lee AH. 2013. Skeletochronology. In: Padian K, and Lamm E-T,
1376 eds. *Histology of fossil tetrapods - Advancing methods, analysis and interpretation*. Berkeley,
1377 Los Angeles, London: University of California Press, 195-215.

1378 Zedda M, Lepore G, Manca P, Chisu V, and Farina V. 2008. Comparative bone histology of
1379 adult horses and cows. *Journal of Veterinary Medicine Series C* 37:442–445.

1380 Zylberberg L, Traub W, Buffrénil V de, Allizard F, Arad T, and Weiner S. 1998. Rostrum of a
1381 toothed whale: ultrastructural study of a very dense bone. *Bone* 23:241-247.

1382

1383 **Figure captions**

1384 **Figure 1: Typical mammalian bone tissue as observed in large mammals such as cervids.**

1385 Red bars indicate area and plane of sectioning. Histological images B), E), and I) in linear
1386 polarised light, C) in crossed polarised light and with additional use of lambda
1387 compensator, and F) in crossed polarised light. A) Life reconstruction of the cervid
1388 *Megaloceros giganteus* ("Knight Megaloceros" by Charles R. Knight, courtesy of the
1389 American Museum of Natural History via Wikimedia Commons -
1390 http://commons.wikimedia.org). B, C) Bone cortex of a tibia of *Megaloceros giganteus*
1391 specimen NMING:F21306/14 displaying an endosteal lamellar layer (innermost part of
1392 the cortex) and reticular as well as plexiform fibrolamellar primary bone with growth
1393 marks. Note that the primary bone is pervaded by secondary Haversian systems in the
1394 inner third of the bone cortex. White arrows indicate lines of arrested growth. Occurrence
1395 of LAGs indicated by black/white arrows and the outer circumferential layer (OCL) by
1396 white brackets. D) Photograph of *Pudu puda* ("Pudupuda hem 8 FdoVidal Villarr
1397 08Abr06-PhotoJimenez", courtesy of Jaime E. Jimenez via Wikimedia Commons -

1398 http://commons.wikimedia.org). E, F) Bone cortex of a femur of *Pudu puda* specimen
1399 NMW 60135 displaying an endosteal lamellar layer and mainly plexiform fibrolamellar
1400 bone. G) Reconstruction of *Paraceratherium* ("Indricotherium11", Courtesy of Dmitry
1401 Bogdanov via Wikimedia Commons - http://commons.wikimedia.org). H) Cross-section
1402 of a rib of *Paraceratherium* sp. specimen MTA-TTM 2006-1209. Red rectangle indicates
1403 area of dense Haversian bone magnified in I).

1404 **Figure 2: Phylogeny of Mammaliamorpha focussing on groups discussed,** based on Luo et
1405 al. (2005), Luo et al. (2011), Meredith et al. (2011), and O'Leary et al. (2013).
1406 Notoungulates and Pantodonta are not included given their controversial systematic
1407 position.

1408 **Figure 3: Femoral bone cortex of marsupials.** Histological images A) and D) in linear
1409 polarised light and B), C), E), and F) in crossed polarised light. A, B) Outer bone cortex
1410 of adult *Didelphis albiventris* specimen PIMUZ A/V 5279. Note the occurrence of simple
1411 primary longitudinal vascular canals and primary osteons in mainly parallel-fibred bone
1412 tissue. C) Inner bone cortex of the same specimen displaying a distinct endosteal lamellar
1413 layer. D, E) Bone cortex of adult *Lutreolina crassicautada* specimen PIMUZ A/V 5275.
1414 F) Inner cortex of same specimen. Note the occurrence of primary longitudinal vascular
1415 canals and primary osteons as well as Haversian systems within the parallel-fibred bone.

1416 **Figure 4: Histological features of the femur of *Deinogalerix* sp.** A) Life reconstruction of
1417 *Deinogalerix koenigswaldi* in comparison to the extant hedgehog *Erinaceus* (modified
1418 from Agustí & Antón, 2002). B) Adult right femur (specimen RGM.178017) in anterior
1419 view. Red bar indicates area and plane of sectioning. C) Lateral bone cortex in crossed

polarised light showing parallel-fibred bone and 5 LAGs. Occurrence of LAGs indicated by white arrows.

Figure 5: Bone cortex of *Hippopotamus minor* femora. A) Life reconstruction (from van der Geer et al., 2010; drawing: Alexis Vlachos) of another Mediterranean dwarf hippopotamid from the Middle Pleistocene of Crete. Since no life reconstruction of *Hippopotamus minor* is available, we here show the one of *Hippopotamus creutzburgi*. Histological images B), and C) in linear polarised light, D) in crossed polarised light. B) Small juvenile specimen CKS 110/B. C) Intermediate sized juvenile specimen CKS 122/B showing reticular to plexiform vascularised bone. Note that the central part mainly consists of reticular bone. D) Outer bone cortex of large juvenile specimen CKS 117 showing mainly parallel-fibred bone. Black and grey areas indicate zones of recrystallisation due to diagenetic alteration of bone tissue.

Figure 6: Histological features of *Sinomegaceros yabei*, the megacerine deer from the Pleistocene of Japan. Histological images in linear polarised light of an adult femur (OMNH QV-4062) depicting A) the whole cross-section and B) a close-up of the outer cortex. The red bar in A) localizes the approximated position of the section on the life reconstruction (courtesy of Hirokazu Tokugawa), and the red rectangle indicates the area of the close-up. B) Note that seven LAGs are visible, as indicated by white arrows.

Figure 7: Bone histology of fossil island rodents. Histological images A) and D) in linear polarised light, B) and E) in crossed polarised light, and C) and F) in crossed polarised light with additional use of lambda compensator. A-C) Adult *Mikrotia* sp. femur (specimen RGM.792085) showing disorganised, mainly parallel-fibred/lamellar bone in its centre. D-F) Adult femur of *Leithia* sp. specimen NMB G 2160 displaying lamellar

bone being pervaded by longitudinal to radial primary osteons and large irregularly shaped and partially oblique secondary osteons.

Figure 8: Bone histology of fossil ochotonids. A) Life reconstruction of *Prolagus sardus* ("Prolagus3", courtesy of Wikimedia Commons - http://commons.wikimedia.org). Histological images B), D), F) in linear polarised light, C) in crossed polarised light with additional use of lambda compensator, and E) in crossed polarised light. B, C) Lateral cortex of *Prolagus oeningensis* femur PIMUZ A/V 4532 showing fibrolamellar bone partially pervaded by irregular secondary osteons in the inner part and mainly parallel-fibred bone in the central and outer part as well as three LAGs. D) Lateral cortex of *Prolagus imperialis* femur RGM.792096 displaying an identical pattern of bone tissue but five LAGs. E) Posteromedial cortex of juvenile *Prolagus sardus* femur NMB Ty. 4974 showing an area of fibrolamellar bone with a high amount of woven-fibred bone in the inner part and an increasing amount of parallel-fibred bone in the central and outer part of the cortex. F) Outer anterolateral cortex of *Prolagus sardus* femur NMB Ty.12659 displaying five LAGs. Note that the line in the lower third of the cortex is a resorption line (RL) and not a LAG. Occurrence of LAGs indicated by white or yellow arrows.

Table 1(on next page)

Table 1: Material used in this study.

Specimens sampled in this study with ontogenetic stage, geological age, locality of death/fossil site, and specimen number.
Institutional Abbreviations: **CKS** Cyprus Kissonerga collection of the University of Athens; **MTA** Natural History Museum, The General Directorate of Mineral Research and Exploration, Ankara, Turkey; **NMB** Naturhistorisches Museum Basel, Switzerland; **NMING** National Museum of Ireland - Natural History; **NMW** Naturhistorisches Museum Wien, Austria; **OMNH** Osaka Museum of Natural History, Japan; **PIMUZ** Paläontologisches Institut und Museum, Universität Zürich, Switzerland; **RGM** Rijksmuseum voor Geologie en Mineralogie (now Netherlands Centre for Biodiversity Leiden)

Table 1: Material used in this study. Specimens sampled in this study with ontogenetic stage, geological age, locality of death/fossil site, and specimen number.

Species	Object	Ontogenetic stage	Geological age; Locality	Specimen number
Didelphis albiventris	Femur	adult	La Plata, Argentina	PIMUZ A/V 5279
"	"	adult	"	PIMUZ A/V 5277
"	"	adult	Ingeniero Mashwitzt, Argentina	PIMUZ A/V 5276
"	"	adult	Ranchos, Argentina	PIMUZ A/V 5278
Lutreolina crassicautada	"	adult	Mar de Ajo, Argentina	PIMUZ A/V 5275
"	"	adult	La Plata, Argentina	PIMUZ A/V 5274
Leithia sp.	Tibia	adult	Pleistocene; Grotta di Maras, Sicily	NMB G 2160
Mikrotia magna	Femur	adult	Late Miocene; Sono Giovo, Gargano	RGM.792083
"	"	adult	"	RGM.792084
"	"	adult	"	RGM.792085
"	"	adult	"	RGM.792086
Prolagus apricenicus	Femur	adult	Late Miocene; San Giovannino, Gargano	RGM.792087
"	"	adult	"	RGM.792088
"	"	adult	"	RGM.792089
"	"	adult	"	RGM.792090
"	"	adult	"	RGM.792091
"	"	adult	"	RGM.702092
"	Humerus	adult	"	RGM.792093
"	"	adult	"	RGM.792094
"	"	adult	"	RGM.792095
Prolagus imperialis	Femur	adult	"	RGM.792096

"	"	adult	"	RGM.792097
"	"	adult	"	RGM.792098
"	"	adult	"	RGM.792099
"	"	adult	"	RGM.792100
"	"	adult	"	RGM.792101
"	Humerus	juvenile	"	RGM.792102
"	"	adult	"	RGM.792103
"	"	adult	"	RGM.792104
Prolagus sardus	Femur	juvenile	Late Pleistocene; Monte San Giovanni, Sardinia	NMB Ty. 4974
"	"	adult	"	NMB Ty. 4977
"	"	adult	Late Pleistocene; Grotta Nicolai, Sardinia	NMB Ty.12656
"	"	adult	"	NMB Ty.12657
"	"	adult	Late Pleistocene; Isola di Tavolara, Sardinia	NMB Ty.12658
"	"	adult	"	NMB Ty.12659
Prolagus oeningensis	Femur	juvenile	Middle Miocene; La Grive, France	PIMUZ A/V 4532
	"	adult		PIMUZ A/V 4532
"	"	adult	"	PIMUZ A/V 4532
"	Humerus	adult	"	PIMUZ A/V 4532
"	"	adult	"	PIMUZ A/V 4532
Megaloceros giganteus	Tibia	adult	Late Pleistocene; Baunmore Townland, Rep. of Ireland	NMING:F21306/14
Sinomegaceros yabei	Tibia	juvenile	Late Pleistocene; Kumaishi-do Cave, Miyama, Hachiman-cho, Gujo City, Gifu Prefecture, Japan	OMNH QV-4067
"	Tibia	adult	"	OMNH QV-4068
"	Femur	juvenile	"	OMNH M-087

"	Femur	adult	"	OMNH QV-4062
Pudu puda	Femur		Tiergarten Schönbrunn, Vienna, Austria	NMW 60135
Hippopotamus minor	"	juvenile	Late Pleistocene; Kissonerga, Cyprus	CKS 110/B
"	"	juvenile	"	CKS 122/B
"	"	subadult	"	CKS 117
Paraceratherium sp.	Rib	adult	Late Oligocene; Gözükizilli, Turkey	MTA-TTM 2006-1209
"	Tibia	adult	"	CKS 215
Deinogalerix sp.	Femur	adult	Late Miocene; Gervasio 1, Gargano, Italy	RGM.178017
"	Humerus	adult	Late Miocene; Chiro 20E, Foggia, Gargano, Italy	RGM.425360

Institutional Abbreviations: **CKS** Cyprus Kissonerga collection of the University of Athens; **MTA** Natural History Museum, The General Directorate of Mineral Research and Exploration, Ankara, Turkey; **NMB** Naturhistorisches Museum Basel, Switzerland; **NMING** National Museum of Ireland - Natural History; **NMW** Naturhistorisches Museum Wien, Austria; **OMNH** Osaka Museum of Natural History, Japan; **PIMUZ** Paläontologisches Institut und Museum, Universität Zürich, Switzerland; **RGM** Rijksmuseum voor Geologie en Mineralogie (now Netherlands Centre for Biodiversity Leiden)

1

Figure 1: Typical mammalian bone tissue as observed in large mammals such as cervids.

Red bars indicate area and plane of sectioning. Histological images B), E), and I) in linear polarised light, C) in crossed polarised light and with additional use of lambda compensator, and F) in crossed polarised light. A) Life reconstruction of the cervid *Megaloceros giganteus* ("Knight Megaloceros" by Charles R. Knight, courtesy of the American Museum of Natural History via Wikimedia Commons - http://commons.wikimedia.org). B, C) Bone cortex of a tibia of *Megaloceros giganteus* specimen NMING:F21306/14 displaying an endosteal lamellar layer (innermost part of the cortex) and reticular as well as plexiform fibrolamellar primary bone with growth marks. Note that the primary bone is pervaded by secondary Haversian systems in the inner third of the bone cortex. White arrows indicate lines of arrested growth. Occurrence of LAGs indicated by black/white arrows and the outer circumferential layer (OCL) by white brackets. D) Photograph of *Pudu puda* ("Pudupuda hem 8 FdoVidal Villarr 08Abr06-PhotoJimenez", courtesy of Jaime E. Jimenez via Wikimedia Commons - http://commons.wikimedia.org). E, F) Bone cortex of a femur of *Pudu puda* specimen NMW 60135 displaying an endosteal lamellar layer and mainly plexiform fibrolamellar bone. G) Reconstruction of *Paraceratherium* ("Indricotherium11", Courtesy of Dmitry Bogdanov via Wikimedia Commons - http://commons.wikimedia.org). H) Cross-section of a rib of *Paraceratherium* sp. specimen MTA-TTM 2006-1209. Red rectangle indicates area of dense Haversian bone magnified in I).

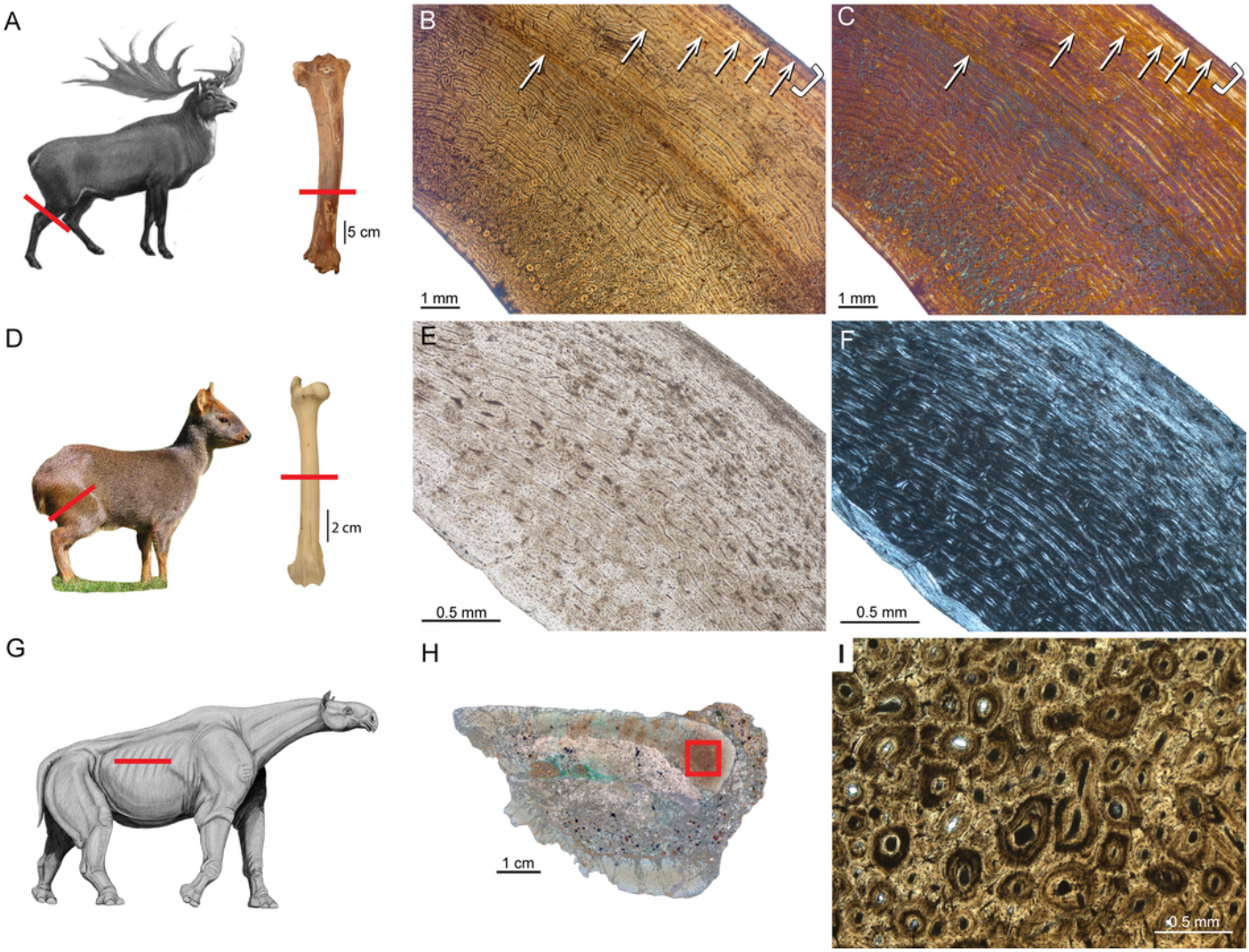
A
5 cm
B
1 mm
C
1 mm
D
2 cm
E
0.5 mm
F
0.5 mm
G
H
1 cm
I
0.5 mm

2

Figure 2: Phylogeny of Mammaliamorpha focussing on groups discussed,

based on Luo et al. (2005), Luo et al. (2011), Meredith et al. (2011), and O'Leary et al. (2013). Notoungulates and Pantodonta are not included given their controversial systematic position.

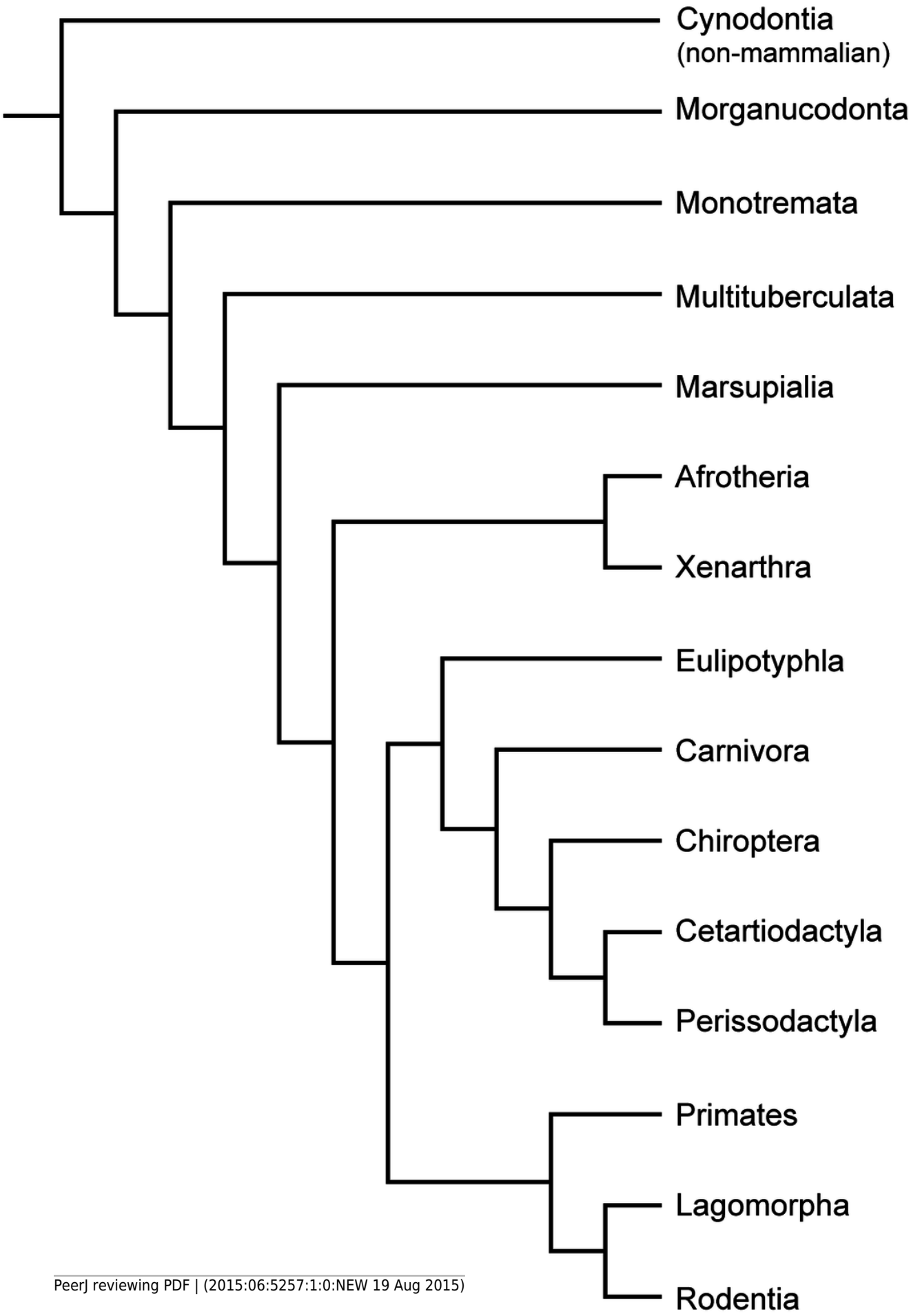
Cynodontia
(non-mammalian)
Morganucodonta
Monotremata
Multituberculata
Marsupialia
Afrotheria
Xenarthra
Eulipotyphla
Carnivora
Chiroptera
Cetartiodactyla
Perissodactyla
Primates
Lagomorpha
Rodentia

3

Figure 3: Femoral bone cortex of marsupials.

Histological images A) and D) in linear polarised light and B), C), E), and F) in crossed polarised light. A, B) Outer bone cortex of adult *Didelphis albiventris* specimen PIMUZ A/V 5279. Note the occurrence of simple primary longitudinal vascular canals and primary osteons in mainly parallel-fibred bone tissue. C) Inner bone cortex of the same specimen displaying a distinct endosteal lamellar layer. D, E) Bone cortex of adult *Lutreolina crassicautada* specimen PIMUZ A/V 5275. F) Inner cortex of same specimen. Note the occurrence of primary longitudinal vascular canals and primary osteons as well as Haversian systems within the parallel-fibred bone.

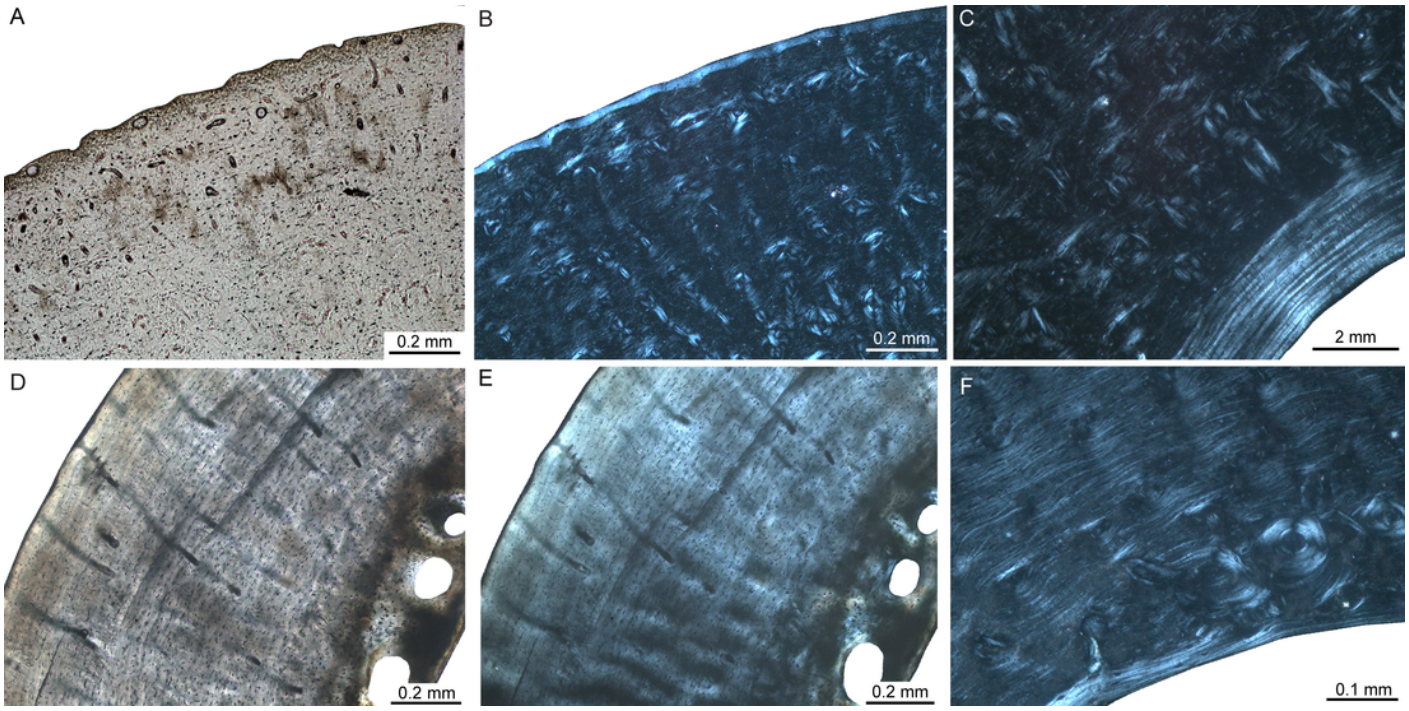

4

Figure 4: Histological features of the femur of *Deinogalerix* sp.

A) Life reconstruction of *Deinogalerix koenigswaldi* in comparison to the extant hedgehog *Erinaceus* (modified from Agustí & Antón, 2002). B) Adult right femur (specimen RGM.178017) in anterior view. Red bar indicates area and plane of sectioning. C) Lateral bone cortex in crossed polarised light showing parallel-fibred bone and 5 LAGs. Occurrence of LAGs indicated by white arrows.

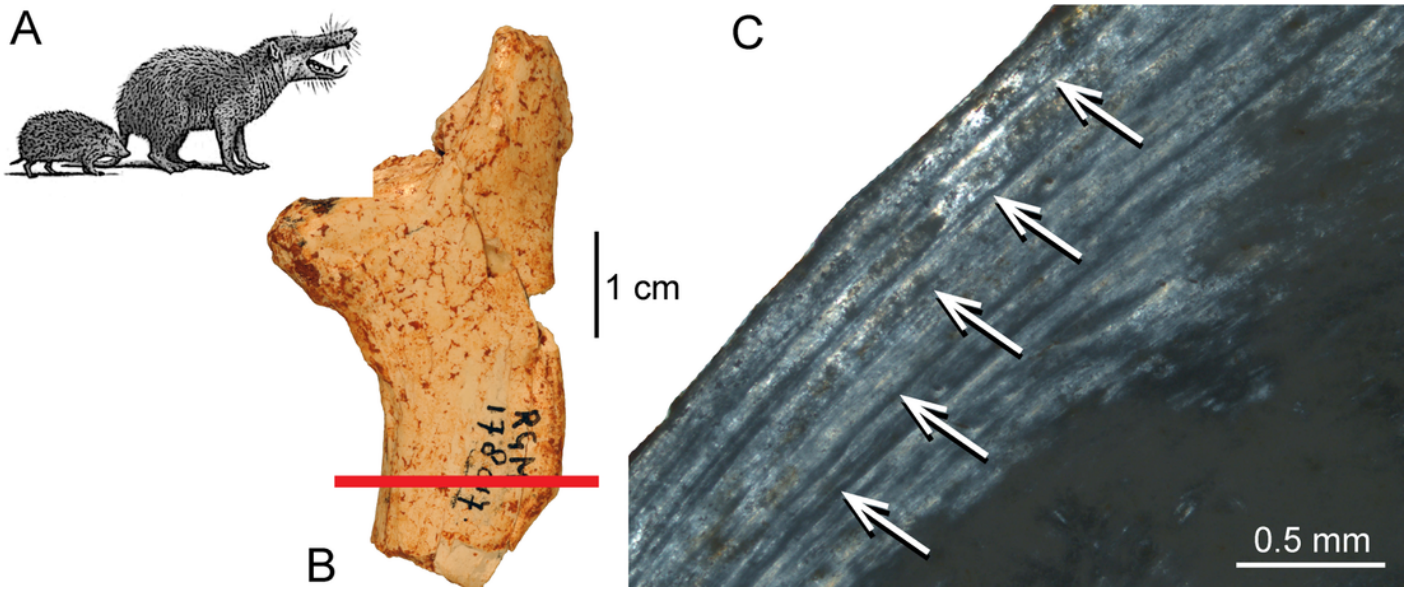

5

Figure 5: Bone cortex of *Hippopotamus minor* femora.

A) Life reconstruction (from van der Geer et al., 2010; drawing: Alexis Vlachos) of another Mediterranean dwarf hippopotamid from the Middle Pleistocene of Crete. Since no life reconstruction of *Hippopotamus minor* is available, we here show the one of *Hippopotamus creutzburgi*. Histological images B), and C) in linear polarised light, D) in crossed polarised light. B) Small juvenile specimen CKS 110/B. C) Intermediate sized juvenile specimen CKS 122/B showing reticular to plexiform vascularised bone. Note that the central part mainly consists of reticular bone. D) Outer bone cortex of large juvenile specimen CKS 117 showing mainly parallel-fibred bone. Black and grey areas indicate zones of recrystallisation due to diagenetic alteration of bone tissue.

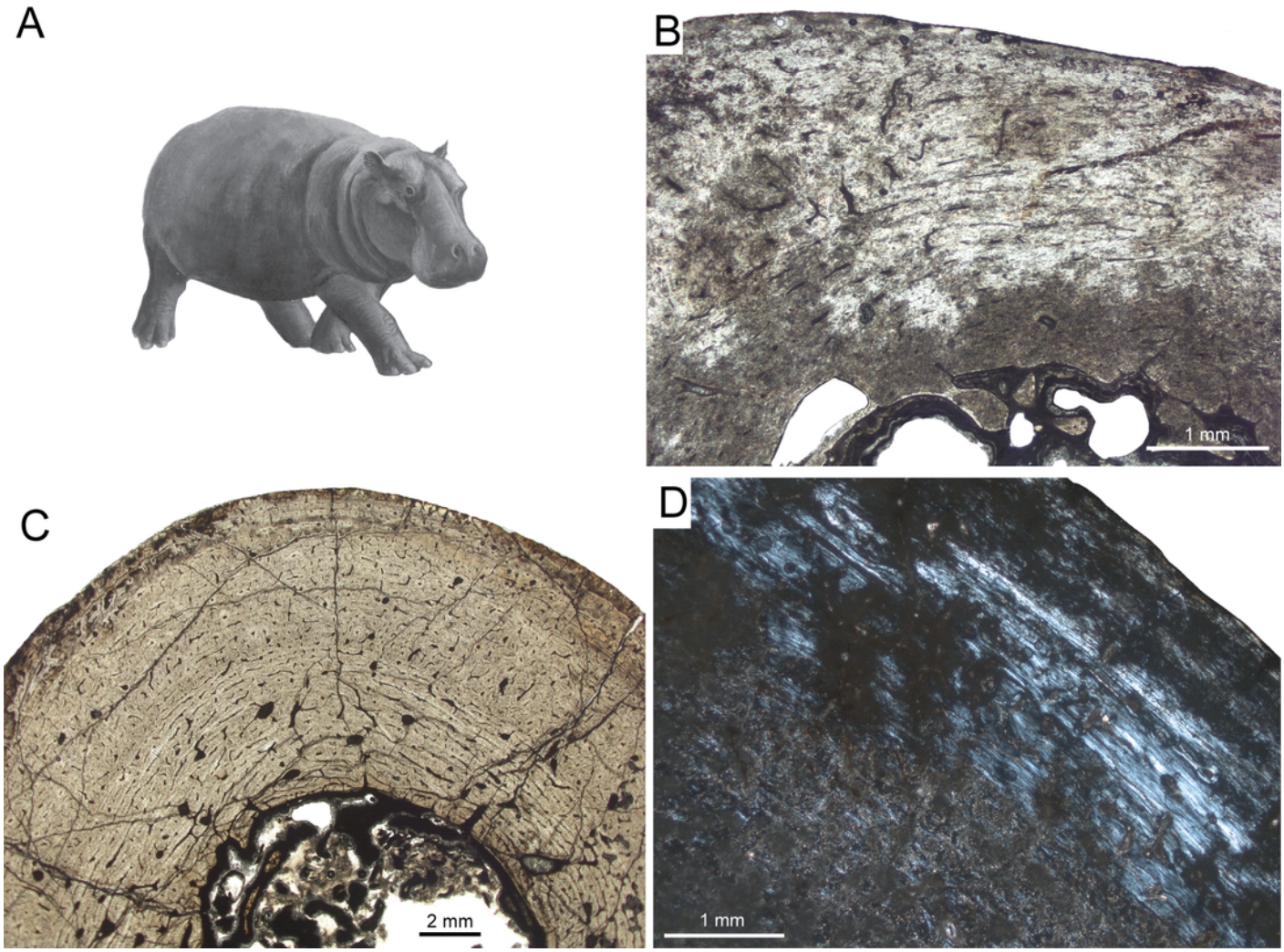
A
B
1 mm
C
2 mm
D
1 mm

6

Figure 6: Histological features of *Sinomegaceros yabei*, the megacerine deer from the Pleistocene of Japan.

Histological images in linear polarised light of an adult femur (OMNH QV-4062) depicting A) the whole cross-section and B) a close-up of the outer cortex. The red bar in A) localizes the approximated position of the section on the life reconstruction (courtesy of Hirokazu Tokugawa), and the red rectangle indicates the area of the close-up. B) Note that seven LAGs are visible, as indicated by white arrows.

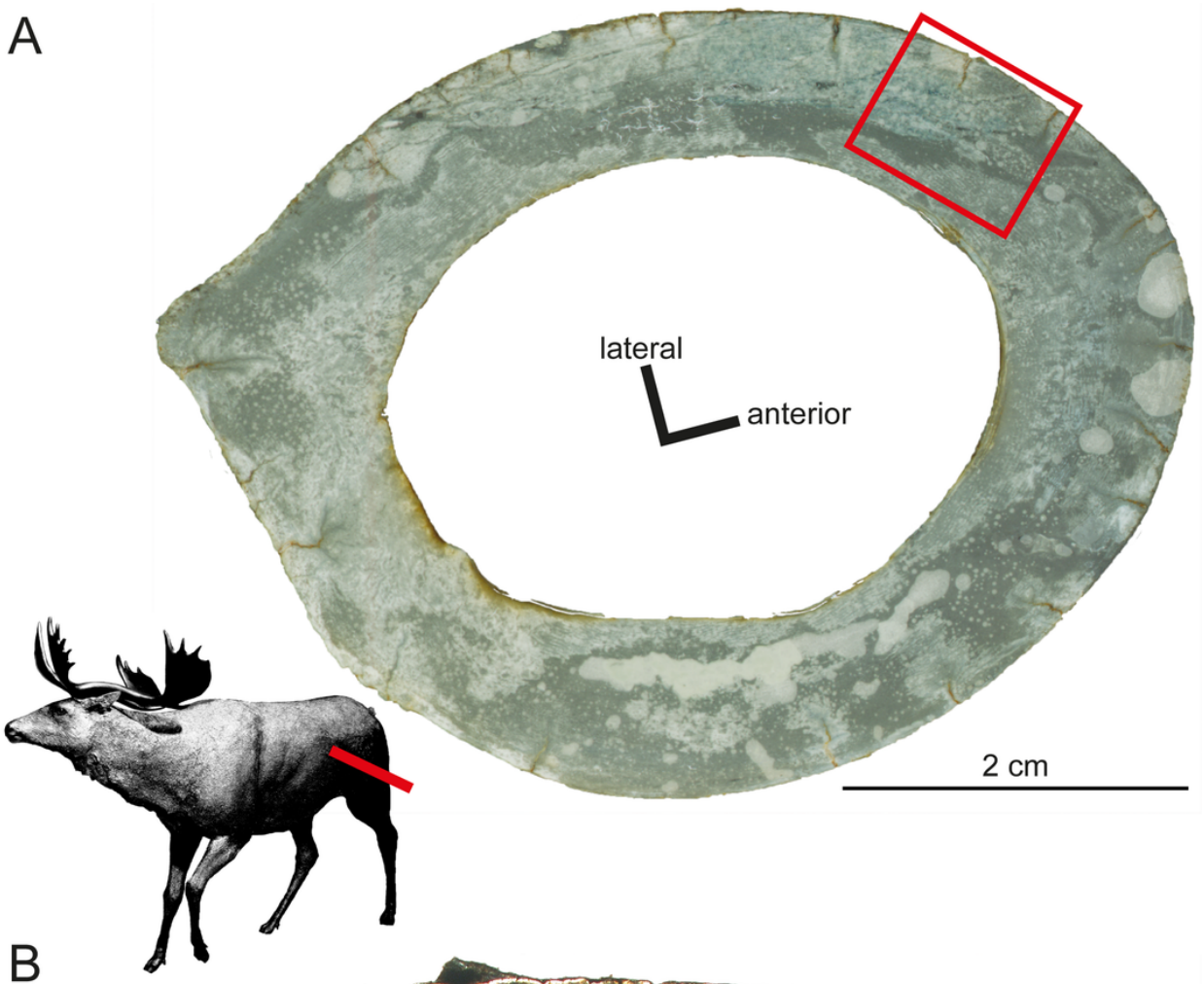
A
lateral
anterior
2 cm

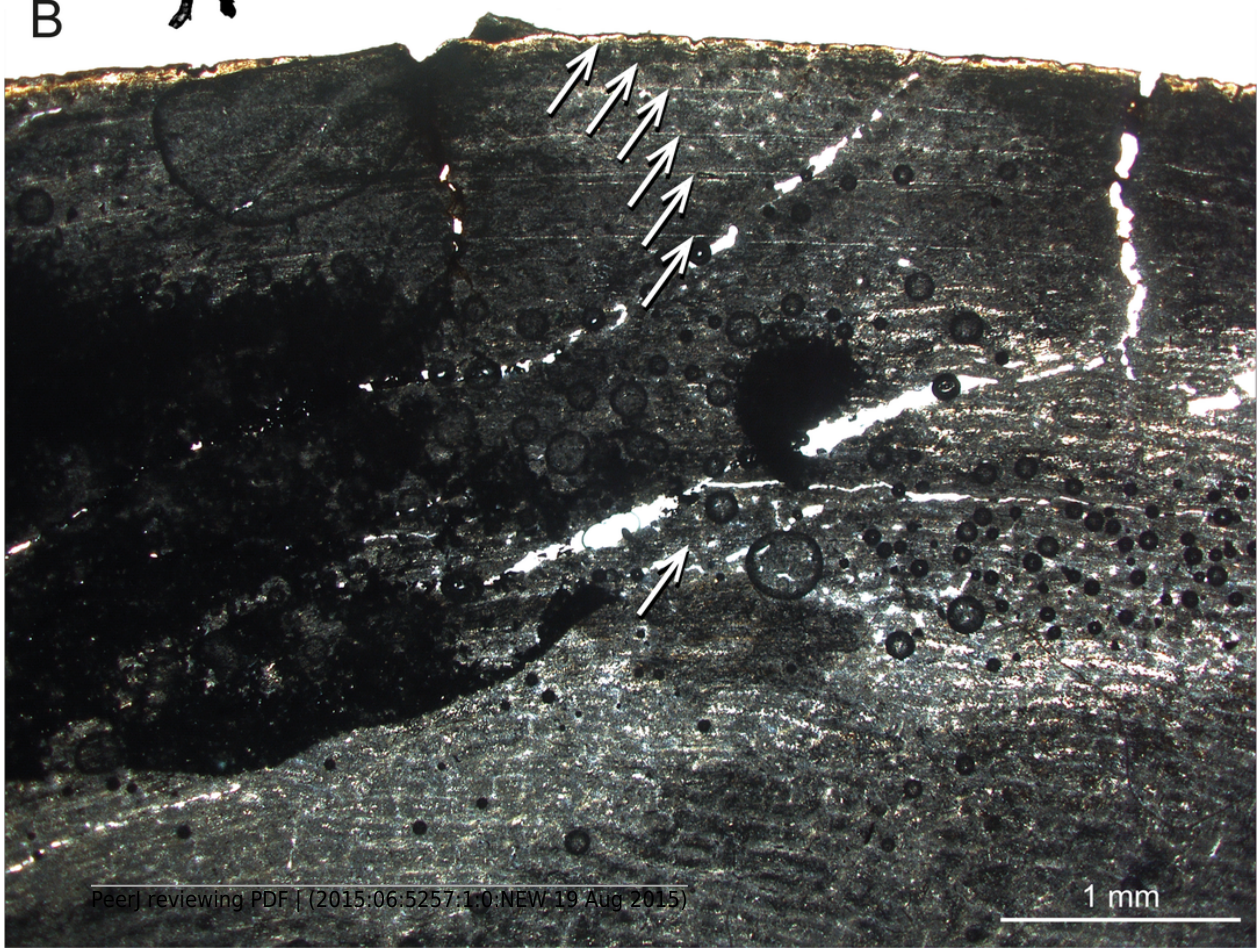
B
1 mm

7

Figure 7: Bone histology of fossil island rodents.

Histological images A) and D) in linear polarised light, B) and E) in crossed polarised light, and C) and F) in crossed polarised light with additional use of lambda compensator. A-C) Adult *Mikrotia* sp. femur (specimen RGM.792085) showing disorganised, mainly parallel-fibred/lamellar bone in its centre. D-F) Adult femur of *Leithia* sp. specimen NMB G 2160 displaying lamellar bone being pervaded by longitudinal to radial primary osteons and large irregularly shaped and partially oblique secondary osteons.

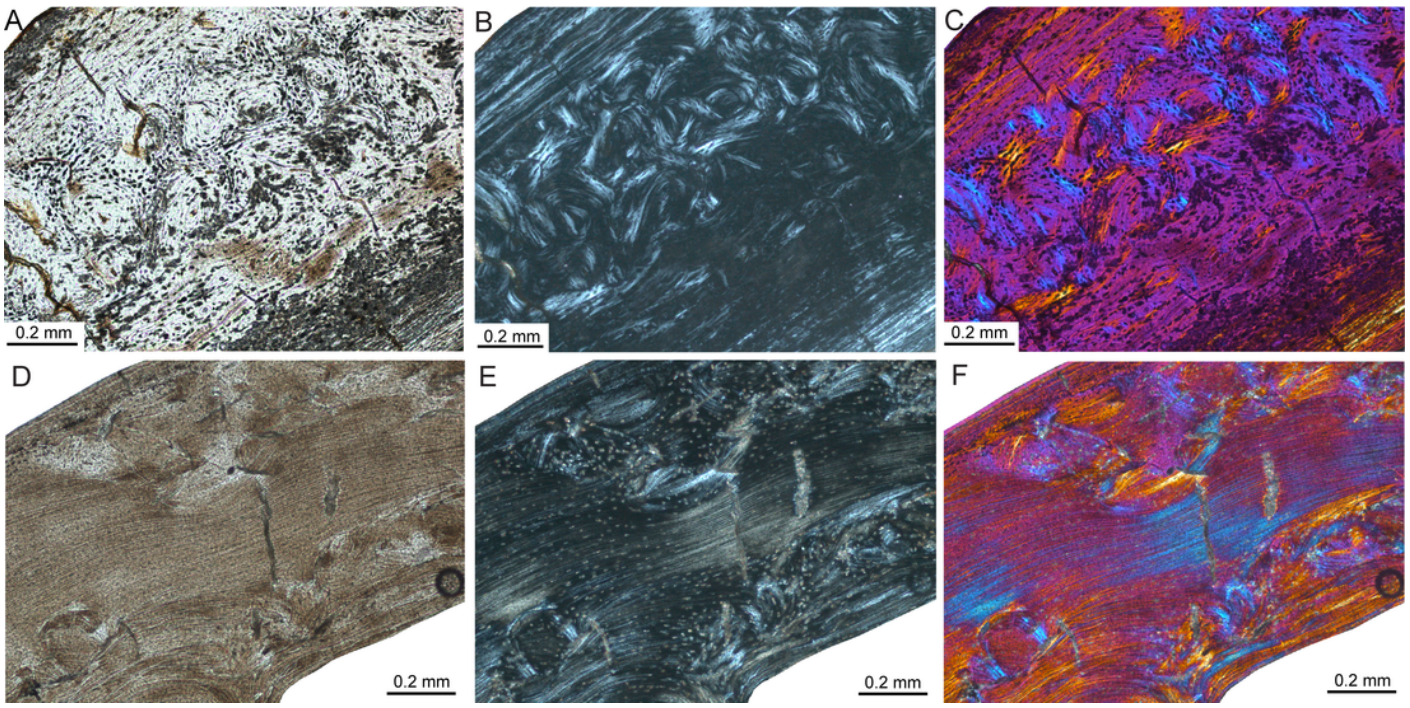

8

Figure 8: Bone histology of fossil ochotonids.

A) Life reconstruction of *Prolagus sardus* ("Prolagus3", courtesy of Wikimedia Commons - http://commons.wikimedia.org). Histological images B), D), F) in linear polarised light, C) in crossed polarised light with additional use of lambda compensator, and E) in crossed polarised light. B, C) Lateral cortex of *Prolagus oeningensis* femur PIMUZ A/V 4532 showing fibrolamellar bone partially pervaded by irregular secondary osteons in the inner part and mainly parallel-fibred bone in the central and outer part as well as three LAGs. D) Lateral cortex of *Prolagus imperialis* femur RGM.792096 displaying an identical pattern of bone tissue but five LAGs. E) Posteromedial cortex of juvenile *Prolagus sardus* femur NMB Ty. 4974 showing an area of fibrolamellar bone with a high amount of woven-fibred bone in the inner part and an increasing amount of parallel-fibred bone in the central and outer part of the cortex. F) Outer anterolateral cortex of *Prolagus sardus* femur NMB Ty.12659 displaying five LAGs. Note that the line in the lower third of the cortex is a resorption line (RL) and not a LAG. Occurrence of LAGs indicated by white or yellow arrows.

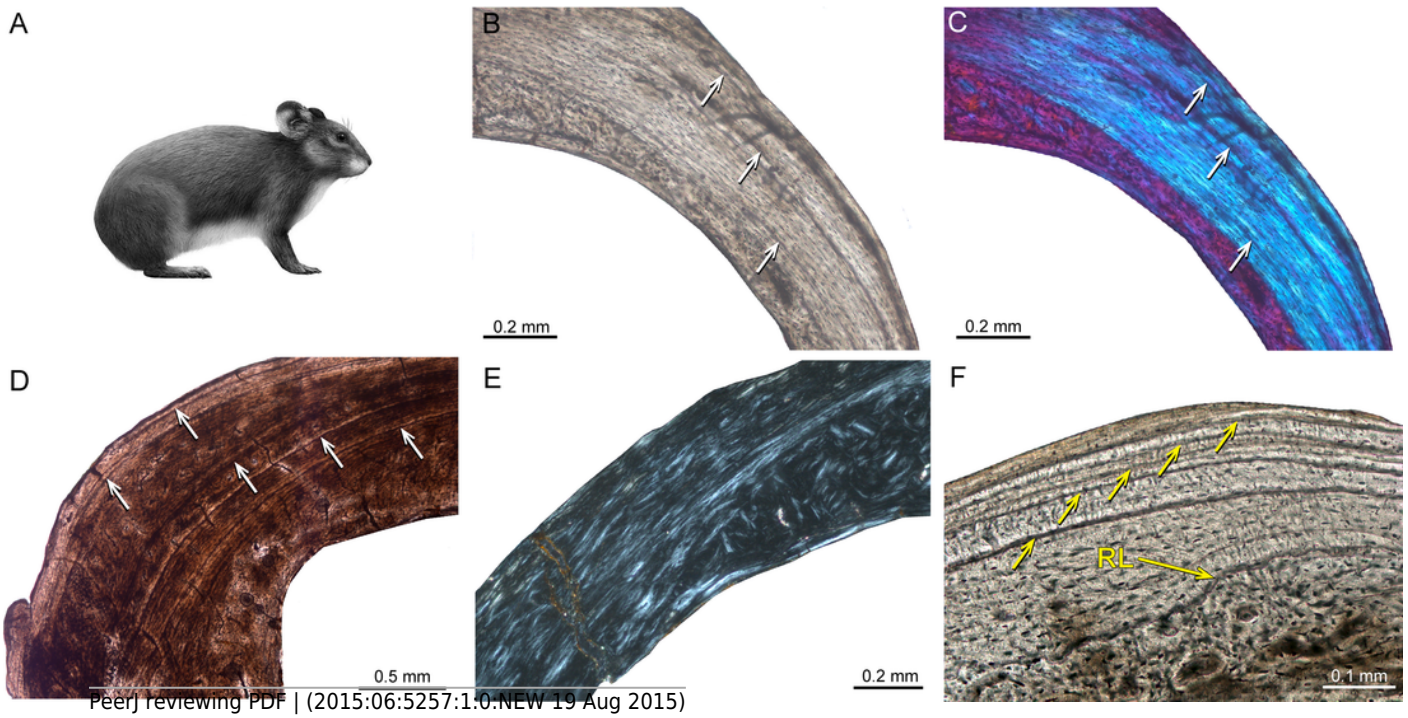

Table 2(on next page)

Table 2: Summary of histological traits of non-mammalian cynodonts and major mammalian clades

(based on material sampled and references cited in the current study). The terminology follows Francillon-Vieillot et al. (1990).

Table 2: Summary of histological traits of non-mammalian cynodonts and major mammalian clades (based on material sampled and references cited in the current study). The terminology follows Francillon-Vieillot et al. (1990).

Histological traits	**Non-mammalian cynodonts**	**Multituberculata and early mammals**	**Monotremata**	**Marsupialia**	**Euarchontoglires**	**Laurasiatheria**	**Afrotheria**	**Xenarthra**
Main primary bone tissue types	fibrolamellar, parallel-fibred, lamellar	fibrolamellar, parallel-fibred, lamellar	fibrolamellar, lamellar	fibrolamellar, parallel-fibred, lamellar	lamellar or parallel-fibred	fibrolamellar	fibrolamellar	fibrolamellar
Main vascularisation patterns	plexiform, laminar, longitudinal, reticular, radial	longitudinal, radial, reticular	longitudinal, radial, reticular, laminar	longitudinal, radial	longitudinal, reticular, radial	longitudinal, reticular, radial, laminar, plexiform	circumferential, longitudinal, reticular, laminar, plexiform	longitudinal, reticular, radial
Lines of arrested growth	present	present	not documented	present	present	present	present	present
Remodelling	Haversian bone	not documented	Haversian bone	Haversian bone	Haversian bone; rodents: low content of Haversian systems	Haversian bone	Haversian bone	Haversian bone